

**This document was prepared in conjunction with work accomplished under Contract No. DE-AC09-96SR18500 with the U. S. Department of Energy.**

**DISCLAIMER**

**This report was prepared as an account of work sponsored by an agency of the United States Government. Neither the United States Government nor any agency thereof, nor any of their employees, nor any of their contractors, subcontractors or their employees, makes any warranty, express or implied, or assumes any legal liability or responsibility for the accuracy, completeness, or any third party's use or the results of such use of any information, apparatus, product, or process disclosed, or represents that its use would not infringe privately owned rights. Reference herein to any specific commercial product, process, or service by trade name, trademark, manufacturer, or otherwise, does not necessarily constitute or imply its endorsement, recommendation, or favoring by the United States Government or any agency thereof or its contractors or subcontractors. The views and opinions of authors expressed herein do not necessarily state or reflect those of the United States Government or any agency thereof.**

# Simulation Analysis for HB-Line Dissolver Mixing

Si Young Lee

November 2005

Westinghouse Savannah River Company  
Savannah River National Laboratory  
Aiken, SC 29808

---

Prepared for the U.S. Department of Energy  
Under Contract No. DE-AC09-96SR18500



**DISCLAIMER**

This report was prepared by Westinghouse Savannah River Company (WSRC) for the United States Department of Energy under Contract No. DE-AC09-96SR18500 and is an account of work performed under that contract. Neither the United States Department of Energy, nor WSRC, nor any of their employees makes any warranty, expressed or implied, or assumes any legal liability or responsibility for the accuracy, completeness, or usefulness, of any information, apparatus, or product or process disclosed herein or represents that its use will not infringe privately owned rights. Reference herein to any specific commercial product, process, or service by trademark, name, manufacturer or otherwise does not necessarily constitute or imply endorsement, recommendation, or favoring of same by WSRC or by the United States Government or any agency thereof. The views and opinions of the authors expressed herein do not necessarily state or reflect those of the United States Government or any agency thereof.

**Printed in the United States of America**

**Prepared For  
U.S. Department of Energy**

**WSRC-TR-2005-00528**

**Keywords:** Computational Fluid  
Dynamics, Agitator Mixing,  
Flow Patterns,  
Helical Agitator

# **Simulation Analysis for HB-Line Dissolver Mixing**

Si Young Lee

November 2005

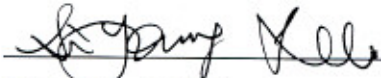
Westinghouse Savannah River Company  
Savannah River National Laboratory  
Aiken, SC 29808

---

Prepared for the U.S. Department of Energy  
Under Contract No. DE-AC09-96SR18500



### Review and Approvals

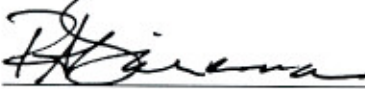
  
\_\_\_\_\_

S. Y. Lee, Author

Eng. Modeling and Simulation Group, SRNL

2/10/06

Date

  
\_\_\_\_\_

R. A. Dimenna, Technical Reviewer

Eng. Modeling and Simulation Group, SRNL

2/10/06

Date


  
\_\_\_\_\_

R. D. Hill, Customer Reviewer

HB-Line Engineering

2-16-06

Date

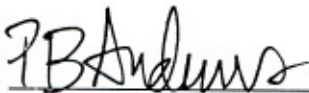
  
\_\_\_\_\_

C. P. Holding-Smith, Manager

Eng. Modeling and Simulation Group, SRNL

2/27/06

Date

  
\_\_\_\_\_

P. B. Andrews, Manager

HB-Line Engineering

3/22/06

Date

## Table of Contents

Abstract.....	1
1 Introduction.....	2
2. Modeling Approach and Analysis .....	6
3. Results and Discussions .....	15
4. Conclusions .....	47
5. References.....	49

## List of Figures

Figure 1.	Geometry of the agitator tank with helical-type four blades and dissolver basket used for the modeling analysis [Dwg. PV180594] .....	3
Figure 2.	Geometrical configurations and real picture view of the clockwise rotating agitator with four 90°-apart helical blades under the nominal conditions used for the analysis .....	4
Figure 3.	Geometrical configurations of the agitator with three 120°-apart flat blades used for the sensitivity analysis .....	5
Figure 4.	Static forces for a single basket in a flowing fluid assuming a solid object with no holes on its wall surface. ....	7
Figure 5.	Configurations of the agitator with four 90°-apart blades as used for the CFD model.....	11
Figure 6.	Configurations of the agitator with three 120°-apart flat blades (Rushton-type blade) as used for the sensitivity analysis .....	12
Figure 7.	Geometrical configurations for 90-deg apart four-blade agitator with helical-type blades submerged in a flat tank as modeled for the present CFD modeling analysis.....	13
Figure 8.	About 250,000 computational nodes of three-dimensional unstructured hybrid meshes for the flat tank with 90-deg helical four-blade agitator as modeled for the present analysis. ....	14
Figure 9.	Maximum fluid velocity as function of the rotational speed of helical pitched agitator submerged in flat tank. ....	19
Figure 10.	Flow patterns around the basket sitting on the bottom of the tank with 1750 rpm agitator speed and 15-liter liquid volume of about 9-in tank level showing that the red zone has the velocity magnitude higher than the critical velocity required for lifting up the basket from the tank floor .....	21
Figure 11.	Comparison of velocity distributions for the entire plane A-A' of the flat tank with 15-liter liquid level and 1750 rpm agitator speed, showing that the red zone has the velocity magnitude higher than the critical velocity required for lifting up the basket from the tank floor .....	22
Figure 12.	Comparison of flow patterns for the entire plane A-A' of the flat tank with 15-liter liquid level and 1750 rpm agitator speed, showing that the red zone has the velocity higher than 0.1 m/sec (0.33 ft/sec).....	23
Figure 12a.	Comparison of pressure distributions near the basket area for the entire plane A-A' of the flat tank with 15-liter liquid level and 1750 rpm agitator speed.....	24
Figure 13.	Comparison of velocity distributions between clockwise and counterclockwise agitator rotations along the vertical line A-A' for the nominal conditions of 1750 rpm and 15-liter tank level .....	25

Figure 14. Velocity vector plot on the horizontal plane crossing the blade for the reference case shown in Table 1 (15-liter tank level and 1750 rpm agitator speed) ..... 26

Figure 15. Three-dimensional velocity vector plot near the agitator blade and dissolver basket from the top of the tank for the reference case shown in Table 1 (15-liter tank level and clockwise 1750 rpm agitator speed) ..... 27

Figure 16. Comparison of wall shear distributions on the surface of the dissolver basket located near the tank bottom for two potential rotating directions of the 1750 rpm agitator submerged in 15-liter tank level, showing that the red region has maximum shear stress (Minimum wall shear required for lifting up the basket due to the fluid motion is about 45 Pa) ..... 28

Figure 17. Flow patterns and contour plots for some physical parameters due to the clockwise rotations of the agitator on the horizontal plane crossing the vertical center of the four-blade agitator for the nominal case (clockwise 1750 rpm agitator speed and 15-liter tank level) ..... 29

Figure 18. Flow patterns and spatial distributions of physical parameters associated with flow circulation pattern and mixing characteristics for the plane crossing the vertical center of the clockwise 1750 rpm mixing agitator submerged in the tank with 15-liter liquid level..... 30

Figure 19. Flow circulation patterns for the plane crossing the center line B-B' of the dissolver basket during the mixing operation of the clockwise 1750 rpm agitator submerged in the tank with 15-liter liquid level..... 31

Figure 20. Flow circulation patterns and characteristics for the horizontal plane crossing the center line C-C' of the clockwise 1750 rpm mixing agitator submerged in the tank with 15-liter liquid level. .... 32

Figure 21. Velocity vector plots for the planes at several different distances ( $x = 0''$ ,  $3''$ ,  $6''$ ,  $8.75''$ , and  $12''$ ) from the clockwise rotated agitator located inside the flat tank (1750 rpm agitator speed with 15-liter tank level)..... 33

Figure 22. Velocity distributions for the planes at several different distances ( $x = 0''$ ,  $3''$ ,  $6''$ ,  $8.75''$ , and  $12''$ ) from the clockwise rotated agitator located inside the flat tank (1750 rpm agitator speed with 15-liter tank level)..... 34

Figure 23. Comparison of velocity distributions between the two rotational directions along the vertical direction from the tank bottom for various horizontal distances from the 1750-rpm helical agitator submerged in the flat tank with 15-liter liquid level..... 35

Figure 24. Velocity distributions near the dissolver basket at the vertical plane crossing the line A-A' for different speeds of the clockwise rotated agitator submerged in 2-liter tank level showing the red zone to be larger than 0.33 ft/sec (min. velocity required for lifting up one dissolver basket is about 2.17 ft/sec)..... 36

Figure 25. Velocity distributions along the vertical line A-A' for different agitator speeds at the horizontal distance of 3 inches from the agitator submerged in the flat tank filled with 15-liter liquid level (clockwise rotated agitator) ..... 37

Figure 26. Comparison of velocity distributions between water and solution along the vertical line A-A' for helical 4-blade agitator at the horizontal distance of 3



inches under the 1750 rpm agitator operation in the flat tank filled with 15-liter liquid level (clockwise rotated agitator)..... 38

Figure 27. Comparison of velocity distributions between two different water levels along the vertical line A-A' for helical 4-blade agitator at the horizontal distance of 3 inches under the 1750 rpm agitator operation in the flat tank filled with 10-liter and 15-liter liquid levels (clockwise rotated agitator) ..... 39

Figure 28. Comparison of velocity distributions between two different rotating directions of agitator along the vertical line A-A' for helical 4-blade agitator at the horizontal distance of 3 inches under the 1750 rpm agitator operation in the flat tank filled with 10-liter liquid level ..... 40

Figure 29. Comparison of velocity flow patterns between two different shapes of the agitators with 1750 rpm operations at the vertical center plane under the same color scale ..... 41

Figure 30. Comparison of velocity contours between two different shapes of the agitators with 1750 rpm operations at the vertical center plane under the same color scale (clockwise rotated agitators)..... 42

Figure 31. Velocity distributions along the vertical line A-A' for different agitator shapes at the horizontal distance of 3 inches under the nominal operating conditions43

Figure 32. Flow circulation patterns and characteristics for the turbulent helical four-blade agitator submerged in the flat HB-Line tank with flow obstacle of dissolver basket..... 46

## List of Tables

Table 1. Nominal reference operating Conditions used for the modeling and analysis .	10
Table 2. Flow conditions driven by the agitator shown in Fig. 1.....	10
Table 3. Maximum and average local velocity magnitudes for three different agitator speeds at the 3-inch distance from the 1750 rpm helical agitator submerged in 15-liter tank level .....	20
Table 4. Comparison of average local velocity magnitudes for three different speeds of the agitator between two types of agitators at the 3-inch distance from the agitator submerged in 15-liter tank level .....	44
Table 5. Summary of results for different rotational speed of helical four-blade agitator submerged in water and solution .....	45

## Abstract

In support of the HB-Line Engineering agitator mixing project, flow pattern calculations have been made for a 90° apart and helical pitch agitator submerged in a flat tank containing dissolver baskets. The work is intended to determine maximum agitator speed to keep the dissolver baskets from contacting the agitator for the nominal tank liquid level. The analysis model was based on one dissolver basket located on the bottom surface of the flat tank for a conservative estimate. The modeling results will help determine acceptable agitator speeds and tank liquid levels to ensure that the dissolver basket is kept from contacting the agitator blade during HB-Line dissolver tank operations.

The numerical modeling and calculations have been performed using a computational fluid dynamics approach. Three-dimensional steady-state momentum and continuity equations were used as the basic equations to estimate fluid motion driven by an agitator with four 90° pitched blades or three flat blades. Hydraulic conditions were fully turbulent (Reynolds number about  $1 \times 10^5$ ). A standard two-equation turbulence model ( $\kappa$ - $\epsilon$ ), was used to capture turbulent eddy motion. The commercial finite volume code, Fluent [5], was used to create a prototypic geometry file with a non-orthogonal mesh. Hybrid meshing was used to fill the computational region between the round-edged tank bottom and agitator regions.

The nominal calculations and a series of sensitivity runs were made to investigate the impact of flow patterns on the lifting behavior of the dissolver basket. At high rotational speeds and low tank levels, local turbulent flow reaches the critical condition for the dissolver basket to be picked up from the tank floor and to touch the agitator blades during the tank mixing operations. This is not desirable in terms of mixing performance. The modeling results demonstrate that the flow patterns driven by the agitators considered here are not strong enough to lift up the dissolver basket for the agitator speeds up to 2500 rpm. The results also show that local velocity magnitudes for the three-blade flat plate agitator are at maximum three times smaller than the helical four-blade one. Table 5 and Table 6 summarize the results.

# 1 Introduction

The HB-line dissolver dissolves metal scrap, which is contained in three porous baskets. The three baskets are connected in series with 1.5-in separation distance by daisy chain, and all of them are submerged into the fluid solution through the edge of the tank so that the scraps inside the baskets are dissolved by the agitated fluid. Each basket is 2-in diameter, 4-in long cylindrical container, and its porous surface consists of 1/16-in holes. The empty basket weighs about 291 gm, and the chain weight is about 26 gm/inch. In this case, the last dissolver basket lies down at the corner of the tank floor, about 4.5 inches away from the tip of the agitator blade as shown in Fig. 1.

As requested by the customer [1], the objective of the present work is to:

- Evaluate the nominal agitator speed in terms of keeping a dissolver basket from contacting the agitator blade during mixing operation in HB-Line tank.
- Perform the sensitivity analysis for different operating conditions such as agitator speeds and shapes, tank levels, and fluid properties.

The present analysis takes a conservative approach by considering a stationary solid object, the last dissolver basket in the chain, on the bottom floor of the HB-line agitator tank. It is modeled as loose and noncohesive solid object of the last empty basket, and liquid flowing over it. This condition will typically occur during a mixing operation after metal scrap inside the basket being dissolved completely by a mechanical agitator. Liquid flow and the stationary dissolver basket are assumed to be statistically in a steady state so that the local flow velocity can be considered the initiator for movement of the basket located on the bottom corner of the tank. As soon as liquid starts flowing, hydrodynamic forces are exerted upon the solid object resting along the wetted perimeter of the fluid-solid system. An increase in flow velocity causes an increase in the magnitude of these forces. Eventually, a condition is reached at which the basket in the movable layer is unable to resist the hydrodynamic forces, gets dislodged, and then starts to move. In reality, it sometimes moves or does not for any given hydraulic condition. The statistical nature of this behavior points to the fact that the flow is turbulent. The onset of initial movement of the basket is predicted by an interfacial force balance on the fluid-solid system.

The primary goal of the present work is to determine whether nominal agitator speed can keep a dissolver basket from contacting the agitator blade during the potential operating conditions with different types of agitators and tank levels. In addition, a series of sensitivity runs is performed to examine the impact of flow patterns on the lifting behavior of the dissolver basket. The results will also help guide the mixing operation of HB-Line dissolver tank.

Schematic diagrams for the HB-line mixing tank system and geometrical configurations for the agitator are illustrated in Figs. 1, 2, and 3 as provided by the customer [1, 2].

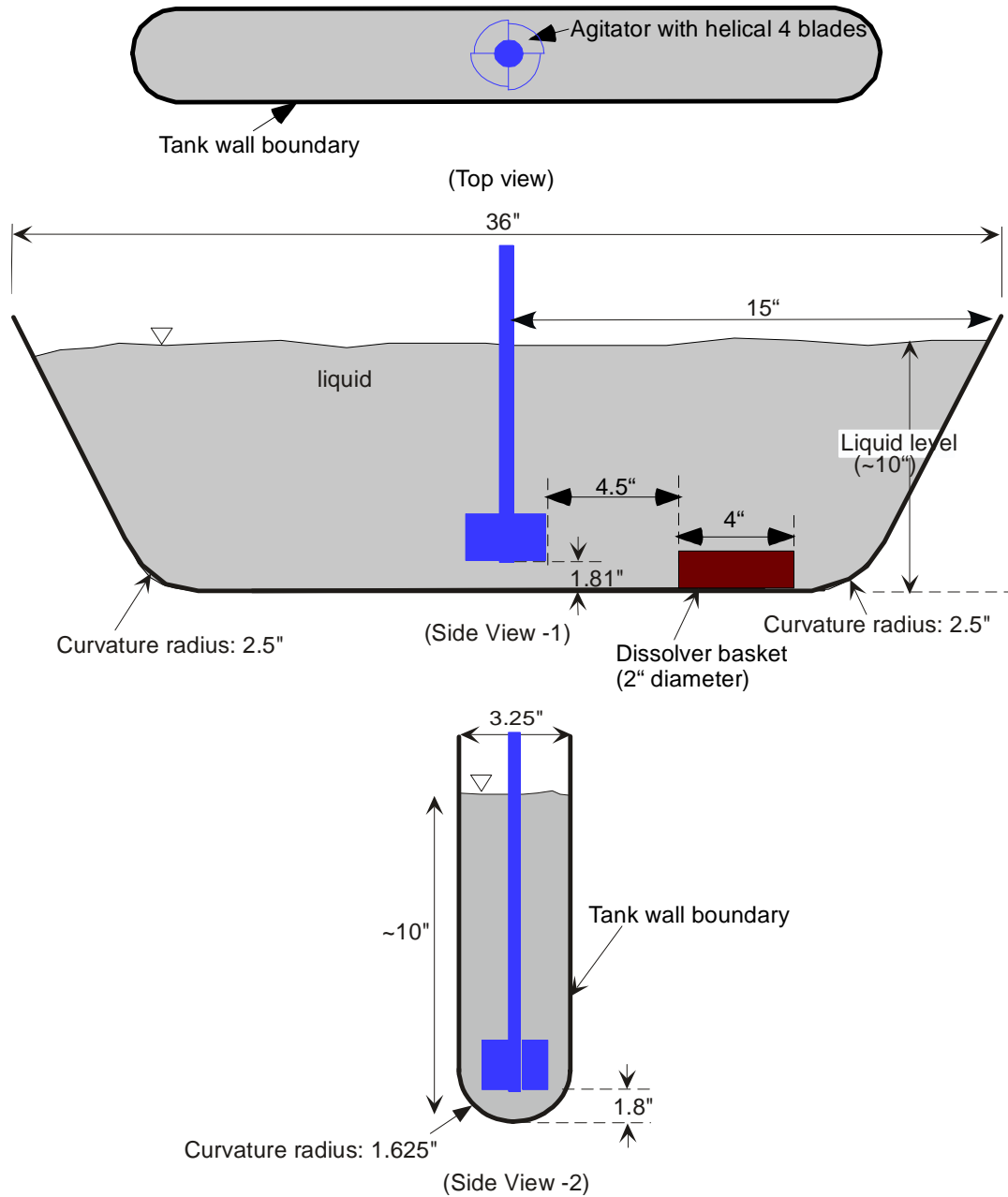


Figure 1. Geometry of the agitator tank with helical-type four blades and dissolver basket used for the modeling analysis [Dwg. PV180594]

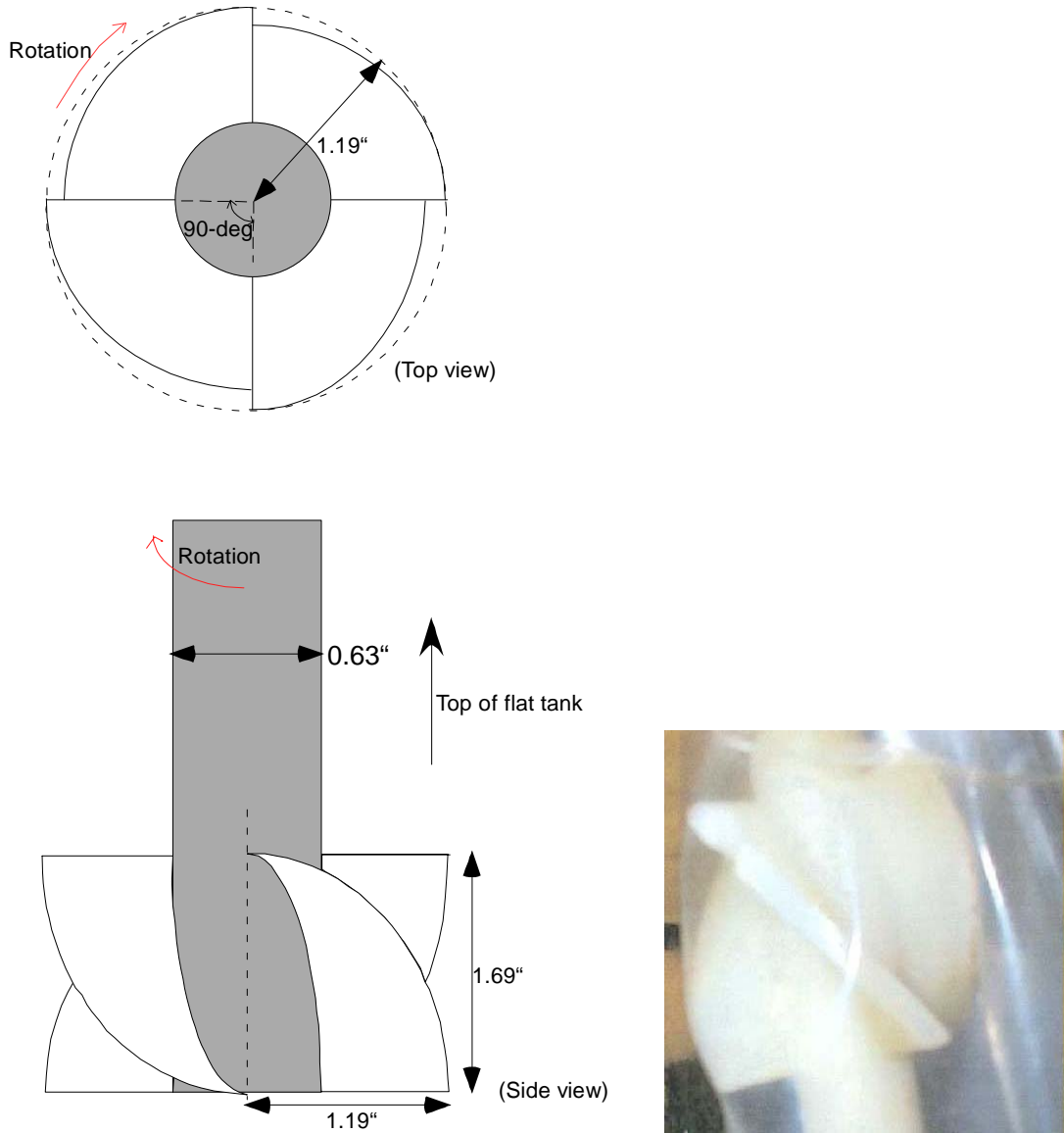


Figure 2. Geometrical configurations and real picture view of the clockwise rotating agitator with four 90°-apart helical blades under the nominal conditions used for the analysis

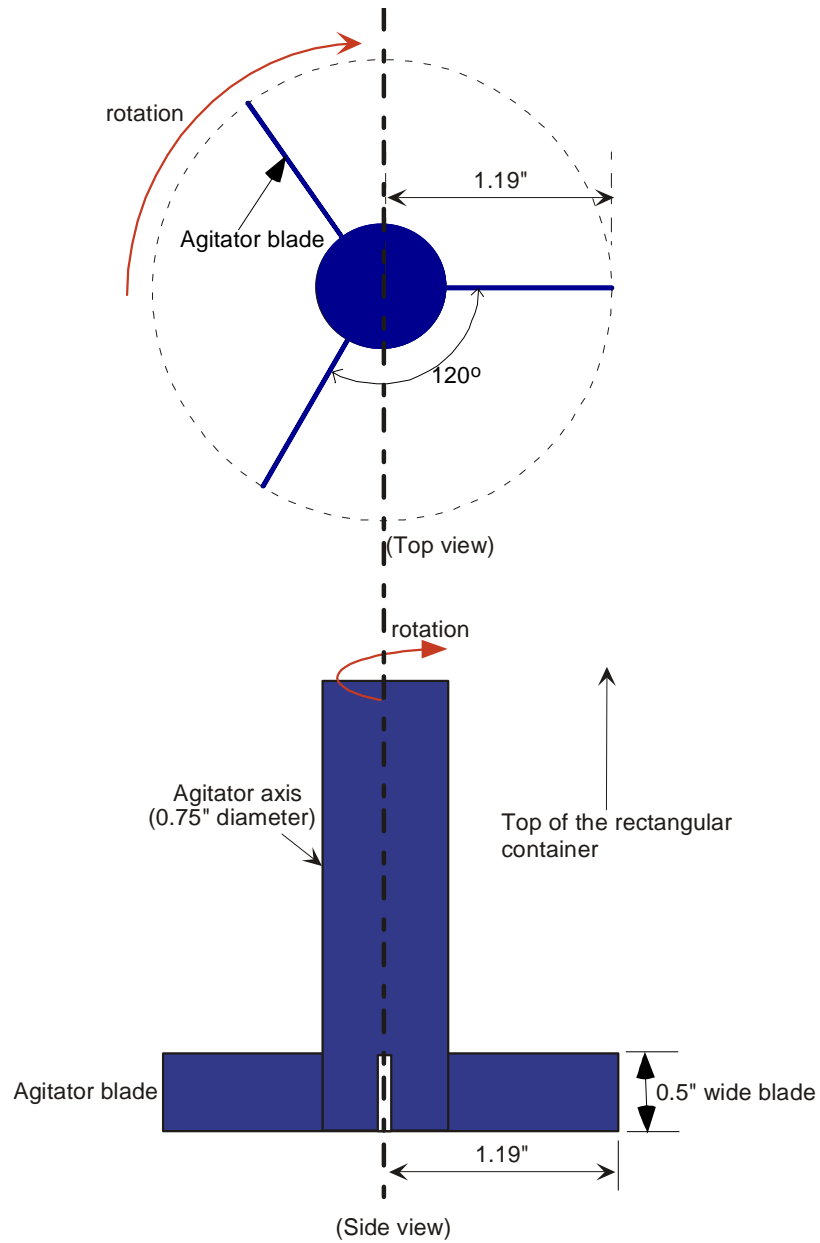


Figure 3. Geometrical configurations of the agitator with three 120°-apart flat blades used for the sensitivity analysis

## 2. Modeling Approach and Analysis

The tank has a thin, flat and rectangular shape. It is about 44" long and 3.25" wide. The tank bottom has round-edged corners with 2.5" curvature radii at both ends of the flat sides and a 1.625" curvature radius for the corner of the round sides. The tank contains several dissolver baskets connected in series by motorcycle chains. The last basket is submerged and located at the bottom corner of the tank. Each basket has the porous wall surface with 1/16-in holes. In this study it is assumed that the external wall surface of the basket has non-porous wall, and it is empty for a conservative estimate of lifting assessment since the scoping calculations show that the empty object with non-porous wall provides higher buoyancy than the submerged object with small holes. Detailed geometrical configurations of the mixing tank as modeled for the analysis are shown in Fig. 1.

The initial movement of one dissolver basket located at the bottom corner of the tank identifies the critical condition or initial lifting. It is usually described by two mechanistic criteria:

- The *critical velocity* criterion considers the impact of the liquid motion on the basket surface such as lifting force due to the gradient of the velocity around the solid object.
- The *critical shear stress* criterion considers the frictional drag of the flow on the basket.

Information gained here will be employed in determining critical conditions to initiate the movement of the basket with no holes on the wall surface, assuming that the presence of 1/16" holes on the surface of the basket is neglected. From these two criteria, the one to provide conservative estimation will be chosen as a performance criterion for the recommendation and guidance of the dissolver mixing operation under the present geometrical configurations because the present work is primarily to determine whether the dissolver basket during the mixing operation is lifted up and touches the agitator blade or not.

### A. Critical Velocity Criterion

The mechanism of basket lifting or pickup in the vicinity of a horizontal surface involves the fluid velocity required to pick up, or prevent settling of, the solid object of a particular size and mass. In this case, it is assumed that an actual mass of the object is measurable, and it has no holes on its wall surface for a conservative estimate since the submerged object without porous surface provides higher buoyancy. The pickup velocity for a solid object lying on a horizontal bottom surface, as shown in Fig. 4, is evaluated from a balance of forces induced by or associated with a horizontal flow of fluid.

The condition of incipient movement for one noncohesive, loose, solid object is described in terms of the forces acting on the particle. The driving force for initial movement is the resultant of the hydrodynamic lifting force,  $F_L$ , and the submerged weight of basket object,  $W_B$ , for a given hydrostatic pressure,  $P_s$ . Atmospheric mass and volume of the basket are  $m_B$  and  $V_B$ , respectively.

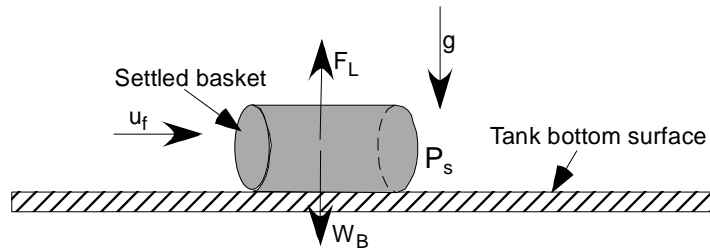
A particle such as shown in Fig. 4 is subject to an upward lifting force  $F_L$ , the Bernoulli force acting on the surface area ( $A_B$ ) of the object where



$$F_L = \left( P_s + \frac{1}{2} \rho_f u_f^2 \right) A_B, \quad (1)$$

and a downward force equal to the static pressure  $P_s$  and the particle weight,

$$\begin{aligned} F_D &= P_s A_B + W_B \\ &= P_s A_B + (m_B - V_B \rho_f) g \end{aligned} \quad (2)$$



- $P_s$  = static pressure
- $W_B$  = basket weight
- $F_L$  = upward lifting force due to the fluid motion driven by the agitator
- $u_f$  = local fluid velocity near the basket
- $g$  = acceleration due to gravity

Figure 4. Static forces for a single basket in a flowing fluid assuming a solid object with no holes on its wall surface.

Hydrostatic pressure acts on both the top and bottom of the object. At the point at which the basket object would just begin to be lifted up, the upward force equals the downward force, so that equation (1) equals equation (2). The resulting relationship simplifies to

$$u_f = \sqrt{\frac{2g}{A_B} \left( \frac{m_B}{\rho_f} - V_B \right)}. \quad (3)$$

Rotational motion of the object is negligible since this approach provides conservative estimate in terms of critical lifting velocity. It should be noted that the model neglects static friction between the surface and an object at rest. In theory, the velocity required to overcome friction can be considerably greater than that derived from this model, which accounts solely for weight and lifting force of the solid object due to fluid momentum. In this case, the liquid level parameter is assumed to be only weakly related to the critical velocity. To apply Eq. (3) to the present work, it is also assumed that for each basket size, a certain “critical velocity” exists, below which the basket will experience sedimentation, and above which it will be lifted up from the tank floor. When the current nominal conditions as provided in Table 1 are applied to Eq. (3), minimum critical velocity  $u_f$  requires about 0.66 m/sec (2.2 ft/sec) for lifting up the basket located at the bottom of the tank.

## **B. Critical Shear Stress Criterion**

The stress on basket wall due to shearing action of a flowing fluid was thought to be an important feature of initial scour or the critical condition for initial movement of a submerged basket. The surface friction due to wall shear is the key mechanism for the initial lifting of the submerged object from the tank floor.

The turbulent fluid-wall interaction is evaluated with a standard  $\kappa$ - $\varepsilon$  model. This model computes the turbulent eddy viscosity  $\nu_t$  by solving two transport equations for  $\kappa$  (turbulent kinetic energy) and  $\varepsilon$  (rate of dissipation of turbulent energy). When applying the wall shear mechanism to the lifting evaluation, it is assumed that the turbulent wall shear stress affects the initial scour or lifting-up of the dissolver basket lying at the bottom of the agitator tank. From the force balance, wall shear force on the basket surface due to the agitated fluid motion should be equal to the net basket weight inside the fluid for the initiation of scouring or lifting up the basket submerged in the tank.

$$\tau_{wc} A_B = (m_B - V_B \rho_f) g \quad (4)$$

In Eq. (4),  $\tau_{wc}$  is the critical shear required to the initial scouring or movement of the basket submerged in the agitated fluid of density  $\rho_f$ . When the dissolver basket mass as provided in Table 1 are applied to Eq. (4), minimum wall shear  $\tau_{wc}$  requires about 44.5 Pa for lifting up the basket on the bottom surface of the tank, assuming the static friction against the wall surface to be negligible for a conservative estimation. In the analysis, the basket is assumed to have no pores on its surface. When the basket is assumed to be completely filled with fluid through the porous surface, the corresponding pressure force of about 237 Pa is required for lifting up the basket.

## **C. Modeling Approach**

Based on the performance criteria discussed earlier, a steady-state computational approach was taken to compute flow fields driven by agitator. The main solution methodologies and modeling assumptions were as follows:

- A computational fluid dynamics (CFD) approach was taken, using the commercial code, Fluent<sup>TM</sup> [5].
- A prototypic geometry for the agitator and mixing tank was created with Fluent using a non-orthogonal control volume method.
- The present model was based on the helical pitched four-blade or 120° apart three-blade agitator and tank with internal solid structure.
- The mixing simulations used three-dimensional steady-state, isothermal governing equations with multiple reference frames (MRF).
- For the steady-state model, the top liquid surface was assumed to be stationary and at atmospheric pressure.
- A two-equation standard turbulence model was used.

As mentioned above, the steady-state model assumes that free surface remains stationary at atmospheric pressure since the tank levels considered here are high enough to avoid air pull-through due to vortex formation near the tips of the agitator

blades [4]. According to the literature information, about 6 inches of tank level is required for the prevention of air pull-through from the free surface under the potential operating conditions.

The analysis consists of two major parts. One part is to calculate the reference operating conditions (10-in tank level corresponding to 15 liter tank volume and 1750 rpm agitator speed) to ensure that the model is representative of actual flow patterns and that the dissolver basket is kept from contacting the agitator blade during the mixing operations. The second part is to perform a series of sensitivity analyses for key operating parameters such as liquid level, blade shape, and agitator speed by using the reference model.

The model considers four basic cases with different agitator speeds to flow pattern sensitivity. The four cases consist of two different shapes of agitators with each agitator having two tank levels, 10 and 7.4 inches, corresponding to the fluid volumes of 15 and 10 liters. Two different shapes of agitators as used in the analysis are shown in Figs. 5 and 6. Detailed operating conditions for the model are provided in Table 1.

Computational domains and meshes for the mixing tank filled to a 15-liter tank level are presented in Figs. 7 and 8. Finer nonuniform and hybrid meshes were used in the corner zones and joint sections near the agitator blade where flow direction changes and flow splits might occur. From a nodalization study, an optimum number of about 250,000 nodes was established for the final analysis of the three-dimensional model. As shown in the Fig. 6, very fine nodes, less than 0.1 inch long, were used near the agitator hub and blade regions to capture the high velocity gradient.

The flow for the entire computational domain is assumed to be turbulent to give a reasonable representation of the liquid jet leaving the blade region. All converged solutions were achieved using the segregated and iterative solution technique.

Table 1. Nominal reference operating Conditions used for the modeling and analysis

Operational Parameters		Operating Conditions
Mixing tank dimensions and agitator types	Helical-type four-blade	See Figs. 1 and 2, clockwise rotation (counterclockwise)*
	Flat-type three-blade*	See Figs. 1 and 3
Tank liquid level from the tank bottom		~ 10 inches (corresponding to 15-liter liquid volume)
		~ 7.4 inches *(corresponding to 10-liter liquid volume)
Blade elevation		1.8 inches (above tank bottom)
Rotational speed of agitator		1750, 2000*, 2500* rpm
Liquid density		1.0 gm/cc (water)
		1.5 gm/cc*(solution) [3]
Liquid viscosity		1 cp (water)
		0.761 cp* (solution) [3]
Each dissolver basket weight		290.9 gm [2]
Each dissolver basket size (diameter and length)		2 in OD and 4 in long

Note:\* For sensitivity runs

Table 2. Flow conditions driven by the helical agitator shown in Fig. 2.

Pump Speed (rpm)	Agitator Reynolds number ( $Re_a$ )*	Flow regime stirred by agitator
1750	$1.064 \times 10^5$	Turbulent flow conditions ( $Re_a > 10,000$ )
2000	$1.216 \times 10^5$	
2500	$1.520 \times 10^5$	

Note: \*  $Re_a = \left( \frac{\rho_f N D_B^2}{\mu_f} \right)$ , where N is the revolution of agitator per unit time.

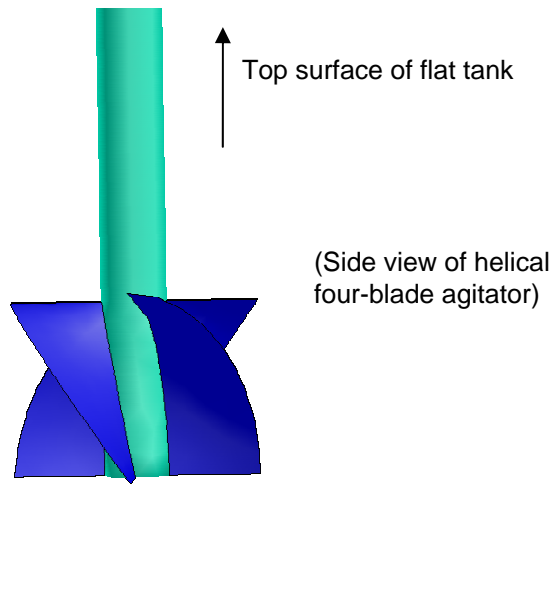
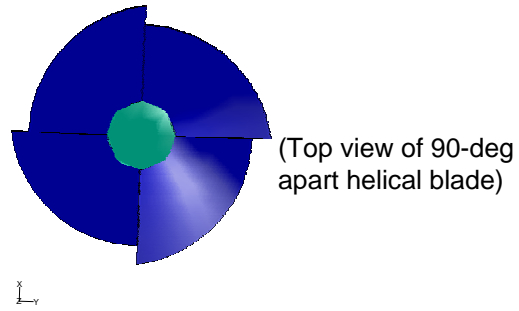


Figure 5. Configurations of the agitator with four 90°-apart blades as used for the CFD modeling calculations

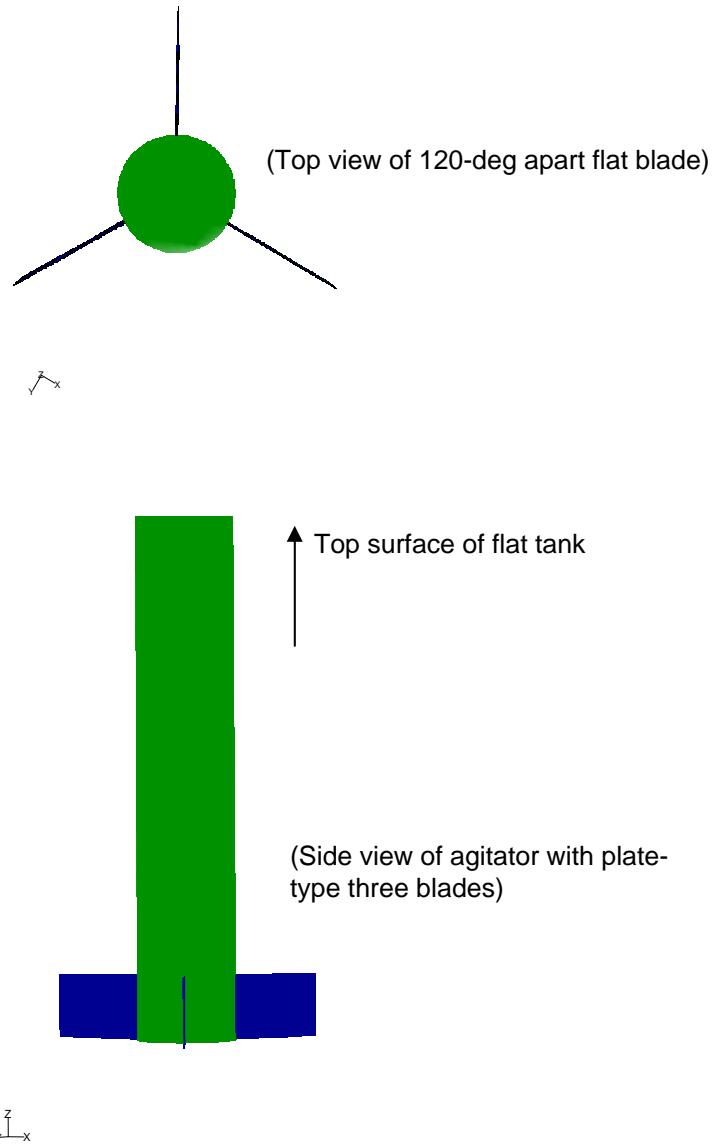


Figure 6. Configurations of the agitator with three 120°-apart flat blades (Rushton-type blade) as used for the sensitivity analysis

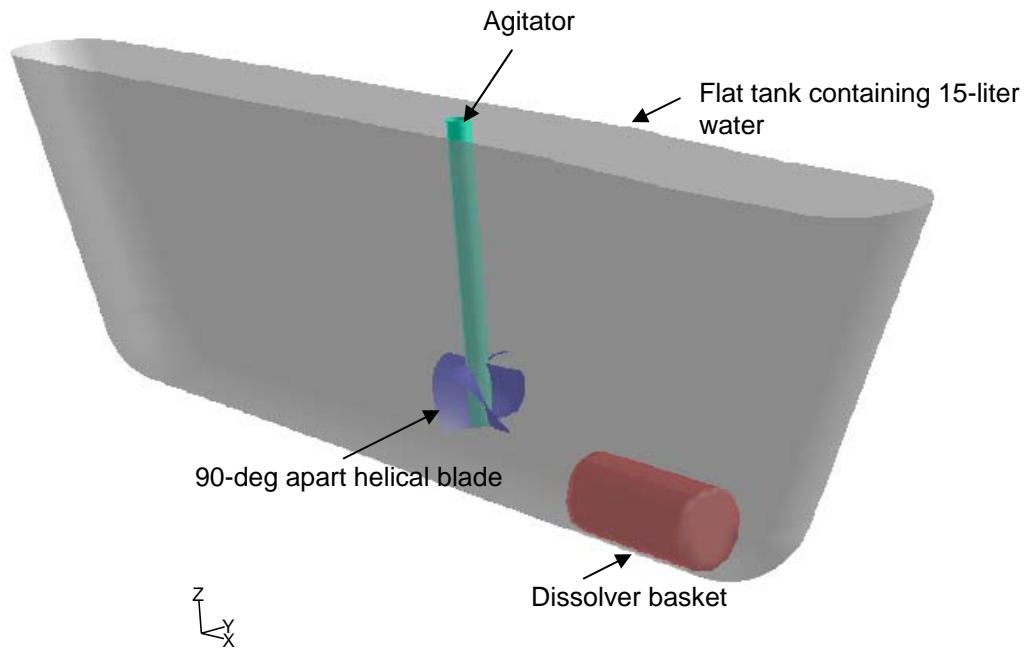


Figure 7. Geometrical configurations for 90-deg apart four-blade agitator with helical-type blades submerged in a flat tank as modeled for the present CFD modeling analysis.

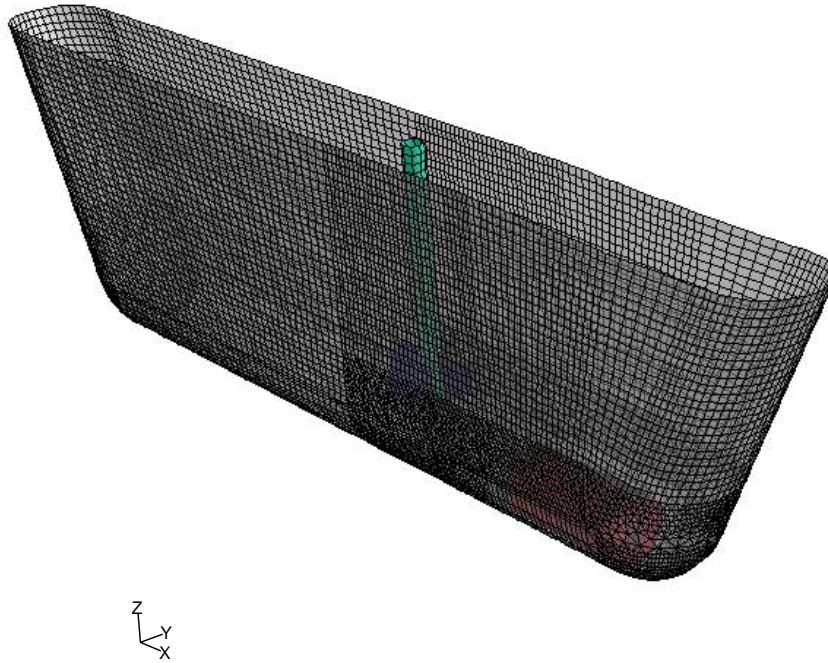


Figure 8. About 250,000 computational nodes of three-dimensional unstructured hybrid meshes for the flat tank with 90-deg helical four-blade agitator as modeled for the present analysis.



### 3. Results and Discussions

Computational results were evaluated by two main criteria for assessing the possibility to lift up the dissolver basket due to the fluid motion of the rotating agitator. The two criteria are critical lifting velocity and minimum wall shear. Critical velocity was used as a criterion to determine whether a given flow condition would result in the suspension of the basket settled on the tank bottom during mixing operations. To ensure conservatism, a shear stress criterion was also applied for the scouring of the basket from the tank bottom because of the interfacial drag at the solid surface. The criteria were quantitatively evaluated under the present operating conditions in the previous section.

Tank liquid level was also a significant parameter. As the tank liquid level becomes lower, local velocity magnitude increases for a given agitator speed since momentum dissipation per unit fluid volume increases. For geometrically similar flow configurations, it can be shown by dimensional analysis that  $P/V$ , the time rate of fluid energy dissipation per unit volume, is governed by the well-established relationship,

$$\frac{P}{V} = \left( \frac{A \rho_f U^3}{2V} \right) \phi_1 = \left( \frac{\rho_f U^3}{H_c} \right) \phi \quad (5)$$

In equation (5),  $\phi_1$  is constant.  $H_c$  is a characteristic length associated with tank liquid level and  $\phi$  is a function of Reynolds number, which is related to the type of flow geometry involved and the particular characteristic velocity employed. The characteristic velocity could be the average velocity  $U$  or the root-mean-squared (rms) fluctuating velocity  $u'$  at a certain position [9].

For all the present flow conditions, the agitator Reynolds number was found to be larger than  $10^5$  as shown in Table 2. The agitator Reynolds number was based on the diameter of agitator and rotational speed as defined in the literature [12], that is,

$$Re_a = \left( \frac{\rho_f U_a D_B}{\mu_f} \right) \quad (6)$$

In equation (6) the agitator speed  $U_a$  is used as the product of rotational speed ( $N$ ) and diameter ( $D_B$ ) of the agitator.

The flow pattern discharged by an agitator depends on both the fluid mass inventory of tank and the agitator rotational speed. The distance through which a fluid element can travel to a remote area is proportional to the rate of kinetic energy dissipation of the fluid element at the point of discharge from an agitator blade [8]. Using well established power correlations for fully turbulent flow stirred by an agitator [9, 10, 11], it can be shown that, for fully-turbulent conditions as shown in Table 2, the power dissipation per unit volume is given by the equation,

$$\left( \frac{P}{V} \right) = \left( \frac{C' \rho_f N^3 D_B^5}{D_T^2 H} \right) \quad (7)$$

In equation (7),  $D_T$  and  $H$  are the diameter and liquid height of an agitator tank. The right-hand side of equation (7) can be equated to the right-hand side of equation (5). Since  $C'$  in equation (7) is constant for turbulent flow, the parameter  $\phi$  should be

constant. Thus, when the geometrical configurations for the mixing system is given for various agitator speeds  $N$ , the resulting equation becomes

$$U = C \frac{ND_B}{(D_T^2 H_c)^{1/3}} = \theta N \quad (8)$$

In equation (8), all the constant terms have been lumped into  $\theta$  for given characteristic lengths of tank and agitator. It is noted that this velocity correlation may have broad applicability, and maintaining a constant value of the parameter  $\theta$  may be a reasonable scale-up criterion in many instances such as small-scale experimental tests and designs. From equation (8), the average velocity outside the agitator discharge zone was found to be proportional to the rotational speed of the agitator, and inversely proportional to the cube root of the tank fluid volume. The maximum fluid velocity discharged by the agitator is found to be proportional to the rotational speed of the agitator as expected. Figure 9 shows the calculated results for different rotational speeds from 1750 rpm to 2500 rpm. The current results were consistent with this relationship over a wide range of agitator speeds, as shown in the figure.

The average local velocity available to pick up solid object stationed at the bottom corner of the tank is also proportional to the agitator speed,  $ND_B$ . The modeling results for different liquid levels under the reference conditions of Table 1 are shown in Table 3. It is noted that local velocity magnitudes for the regions near the basket are much less than the critical velocity required for scouring one dissolver basket.

Flow patterns around the dissolver basket along the center plane of the mixing tank under the nominal operation conditions of 1750 rpm agitator speed with clockwise rotation and 15-liter tank level are shown in Fig. 10. Figure 11 compares velocity distributions for two different rotating directions under the reference operating conditions near the dissolver basket area at the center plane of the tank, indicating that the red zone in the figure has the velocity higher than the minimum velocity of 0.66 m/sec required for lifting up the dissolver basket. The flow pattern results corresponding to the velocity distributions over the agitator mixing region near the settled basket are compared under the same color scaling system in Fig. 12. The corresponding pressure distributions near the basket area under the clockwise and counterclockwise operations are presented in Fig. 12a. The results show that the fluid moves downward along the axis of agitator, rotates around the helical blades, and then moves upward along the side edges of wall boundary after traveling over the basket. It is noted that fluid rotates clockwise near the edge boundary of the blades when the agitator rotates clockwise with 1750 rpm speed. As shown in the figures, maximum velocity magnitude and pressure difference over the basket area under the counterclockwise rotation are 0.15 m/sec and 14 Pa, respectively. These are much smaller than the minimum criteria required for the basket pickup.

As shown in Fig. 13, local velocity magnitude near the basket for the counterclockwise rotating case is much larger than the nominal case of the clockwise motion under the same operating conditions although velocity magnitudes averaged over the entire region are about the same magnitude for the two cases. The nominal rotating agitator with helical blades drives more flow circulation in the vertical direction rather than in the horizontal plane of the agitator as shown in Figs. 14 and 15. The figure shows that the fluid adjacent to the agitator blade moves along the curvature of the blade. The patterns are consistent with the typical literature results for the propeller blades [8].

Wall shear stress or pressure gradient over the basket surface was also evaluated as a pickup criterion of the dissolver basket. In this case, the basket-to-tank surface interactions and the flow effects through 1/16-in pores on the basket wall surface were assumed to be negligible for a conservative estimate since the velocity magnitude via 1/16-in pore due to the pressure force under the potential operating conditions is about 4 mm/sec at 2500 rpm speed [11] and the contact surface area of the basket is large due to the concave shape of the tank floor. The critical shear stress required to scour a 2-in diameter and 4-in long cylindrical object such as the empty dissolver basket was found to be about 44.5 Pa from the force balance between the submerged basket weight and wall shear caused by the fluid motion as shown by Eq. (4). When the basket is filled with fluid, the corresponding pressure force was calculated as about 237 Pa pressure difference. Figure 16 compares wall shear distributions on the surface of the dissolver basket located near the tank bottom for the two different rotating directions of the 1750 rpm agitator submerged in 15-liter tank level, showing that the red region has maximum shear stress. The modeling results clearly show that maximum wall shears on the wall surface of the dissolver basket are far less than the critical shear value of 44.5 Pa necessary for the basket pickup. Therefore, the critical velocity was used as the primary criterion to determine the agitator speed to achieve adequate solid mixing in the tank.

The turbulent flow fields that develop in an agitated tank are generated by the rotational motion of the agitator. Agitator flow phenomena include high-speed discharge flow, blade boundary layers, blade wake regions, boundary layer separation regions, and trailing vortex systems. An understanding of the velocity flow fields is a prerequisite to understanding mixing and key physical parameters such as shear stress, flow fluctuations, and vorticity fields. The vorticity distributions on the agitator blades, as shown in Fig. 17, provide a direct indication of flow field development resulting from the no-slip condition at the blade wall. The fluid particles near the blade wall are accelerated by an imbalance of shear forces.

$$\nabla \cdot \tau = \mu \nabla^2 \vec{v} = -\mu \nabla \times (\nabla \times \vec{v}) = -\mu \nabla \times \omega \quad (9)$$

As shown in equation (9), an unbalanced shear stress can only exist when the vorticity is nonzero. Thus, the existence of vorticity means that a fluid particle is subjected to net viscous forces. Figure 17 shows flow patterns, velocity magnitudes, turbulence intensity, and vorticity fields for the clockwise rotating motions of the 1750 rpm agitator on the horizontal plane crossing the vertical blade center. The results show that the strongest discharge flow fields occur at the agitator blade, and flow fluctuations and vortex motion originate from the tip of the blade. The corresponding spatial distributions of some physical parameters associated with flow circulation pattern and mixing characteristics are shown at the vertical plane crossing the center of the helical four-blade agitator in Fig. 18. Fluid near the rotational axis of the agitator moves downward, and the maximum flow velocity occurs near the tip of the agitator blade. The figure clearly shows that the agitated turbulent flow dissipates from its point of origin at blade tip to the downstream region.

When looking down from the top of the tank, detailed two-dimensional flow patterns near the agitator and dissolver basket at the horizontal plane crossing the basket and agitator blade centers are shown in Figs. 19 and 20. Vertical flow patterns at several different distances from the agitator are shown in Fig. 21. Corresponding snapshots of the fluid velocity distributions are shown in Fig. 22 for the nominal agitator speed and tank level of 1750 rpm and 10 inches (15-liter liquid volume). The red zone in the figures has the fluid domain having velocities higher than the local velocity of 0.17 ft/sec for a 1750 rpm

agitator speed and 10-inch tank level corresponding to 15 liters fluid volume. When the agitator rotates in a clockwise direction, fluid near the rotational axis of the agitator moves downward, and then it is split into two main horizontal directions toward the tank corners along the bottom surface of the tank.

For the reference operating conditions, local velocity distributions along the vertical directions near the basket region are compared between the clockwise and counterclockwise rotations of helically pitched agitator quantitatively in Fig. 23. The calculated results for the nominal clockwise rotation show that maximum local speed for the nominal clockwise rotated agitator over the basket area is about 0.05 m/sec, compared to 0.15 m/sec for the counterclockwise rotation under the same 1750 rpm agitator speed and 15-liter tank level. As shown in the figure, the 1750 rpm agitator speed can not lift up the basket resulting from the fluid motion driven by the agitator regardless of the rotational directions since minimum velocity magnitude of 0.66 m/sec (or 2.17 ft/sec) required for lifting up the dissolver basket is at least about 4 times larger than the maximum local velocity of the basket region.

Sensitivity studies of local flow fields were performed for rotational speeds from 1750 to 2500 rpm, two tank levels, 10 and 7.4 inches, and two different fluids of water and solution. Detailed modeling conditions considered here are provided in Table 1. For three different agitator speeds of 1750, 2000, and 2500 rpm, steady-state calculations of the flow fields were performed to estimate the sensitivity of turbulent flow patterns for each tank level and to examine the possibility for the dissolver basket to contact the agitator blade during tank mixing operations. The sensitivity calculations were performed for the three different speeds at 10-inch tank level representative of a 15-liter fluid volume in the HB-line tank with the agitator rotating in a clockwise direction as viewed from above. As shown in Fig. 24, the results for all the speeds showed that both sides of the agitator had the least active flow zones. The flow patterns did not change significantly as the agitator speed increased. Figure 25 shows the quantitative results for the velocity distributions for various agitator speeds at a local position 3 inches distant from the agitator shaft near the basket region. The results show that all the agitator speeds satisfied the acceptance criterion, which requires that the dissolver basket be not lifted up by the fluid motion to avoid contacting the agitator blade during the agitator mixing.

When tank fluid is switched to the solution, about 50% heavier than the nominal fluid of water, the calculated results show that local velocity magnitude near the dissolver basket is decreased by about 10%, compared to that of the nominal conditions as shown in Fig. 26. The impact of tank liquid level on the flow fields was also evaluated for a given agitating speed in a clockwise rotation. Two different tank levels corresponding to 10 and 15 liters tank volumes were evaluated to estimate the sensitivity of flow patterns to the rotational speed of the agitator. As shown in Fig. 27, local velocity magnitude for the lower tank level of the 10-liter fluid volume is slightly higher than the higher one under the nominal operating conditions other than the tank level. These results are consistent with Eq. (7), which is related to the ratio of power dissipation ( $P$ ) to tank fluid volume ( $V$ ). When the agitator direction is switched from the nominal clockwise to counterclockwise rotation under the tank level corresponding to the 10-liter tank volume, local velocity magnitude near the dissolver basket region is about two times higher than the clockwise operation as compared in Fig. 28. The results show that maximum local flow speed over the basket inside the 10-liter filled tank is about 0.15 m/sec. This is much less than the minimum velocity of 0.66 m/sec required for lifting up the basket.

In the present study, helical four-blade agitator was used as one of the reference operating conditions in Table 1. As shown in Fig. 6, flat-plate three-blade agitator was used to estimate the sensitivity of local flow patterns. The modeling results for the flow patterns are presented in Fig. 29. Figure 30 compares the velocity contours corresponding to the flow patterns for the two types of the agitator blades for the same rotational speed and tank level. The results of Fig. 31 clearly show that local velocity magnitudes for the three-blade agitator are at maximum three times lower than the helical four-blade one. Table 4 presents a summary of the quantitative comparison for those two types of the agitator.

All the above analyses were made with a three-dimensional steady-state turbulence model based on the initial blade selection for the agitator. The modeling results for various pump speeds and different fluids are compared with critical velocities under the nominal tank levels of 15-liter tank volume and helical four-blade agitator in Table 5. Table 6 shows the results for different agitator speeds under the three-blade flat-plate agitator. Overall flow patterns for the nominal clockwise and counterclockwise rotating agitators with helical four blades and a fully-submerged obstacle of the dissolver basket are compared in Fig. 32.

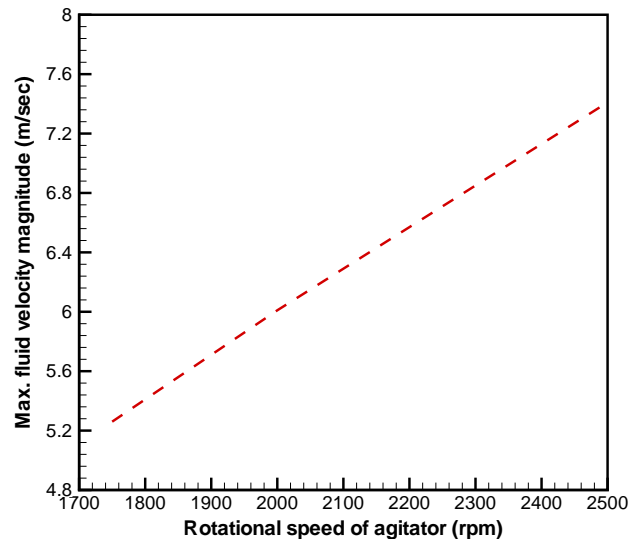
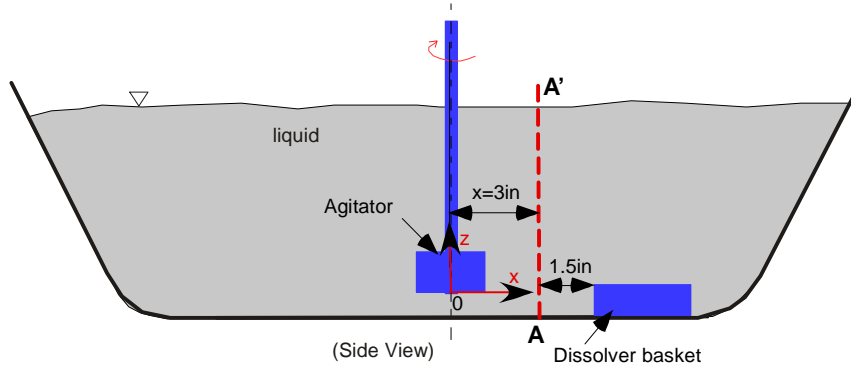


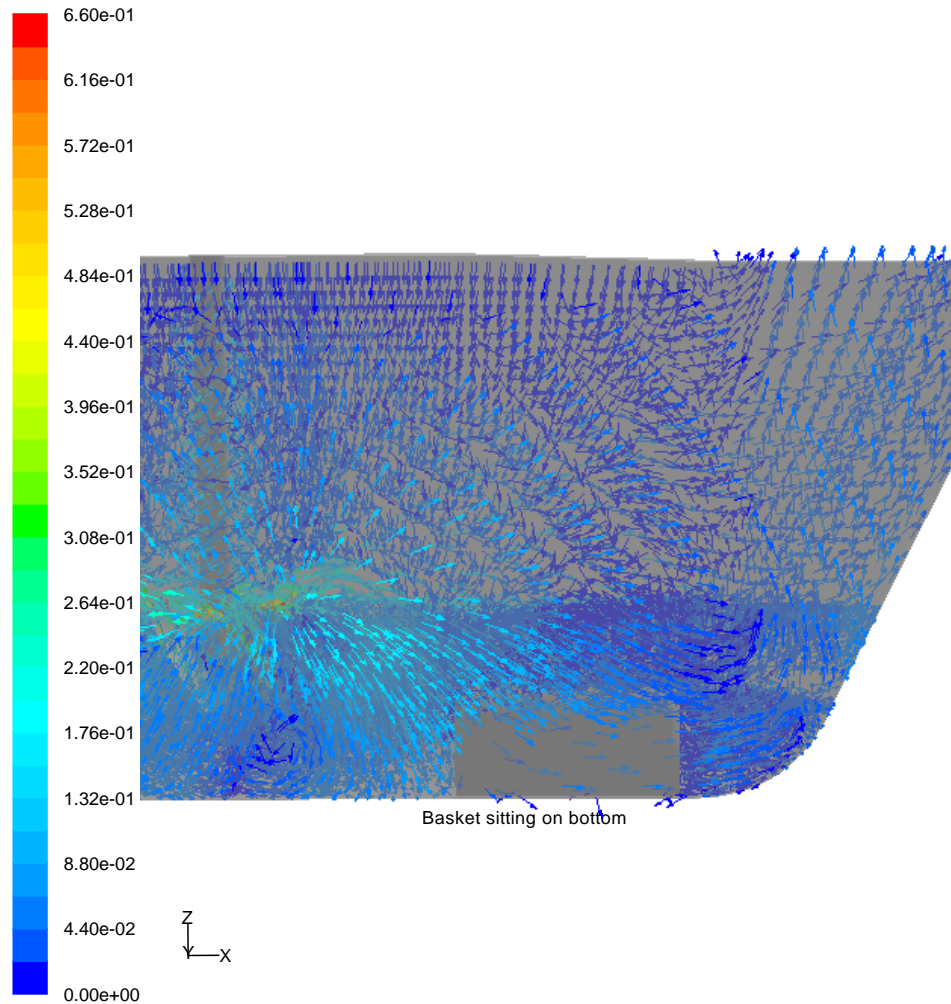
Figure 9. Maximum fluid velocity as function of the rotational speed of helical pitched agitator submerged in flat tank.

Table 3. Maximum local velocity magnitudes near the agitator and at the 3-inch distance from the helical agitator submerged in 15-liter tank level under three different agitator speeds



Agitator speed (rpm)	Max. fluid velocity driven by helical agitator (m/sec)	Max. local velocity at the vertical plane A-A' (m/sec)	Min. critical velocity required for lifting up one basket (m/sec)
1750	5.26	0.086 (0.115)*	0.66
2000	6.01	0.097 (0.150)*	
2500	7.41	0.119 (0.185)*	

Note:\* For counterclockwise rotation



Velocity Vectors Colored By Velocity Magnitude (m/s) Sep 27, 2005  
FLUENT 6.2 (3d, segregated, ske)

Figure 10. Flow patterns around the basket sitting on the bottom of the tank with 1750 rpm agitator speed and 15-liter liquid volume of about 9-in tank level showing that the red zone has the velocity magnitude higher than the critical velocity required for lifting up the basket from the tank floor

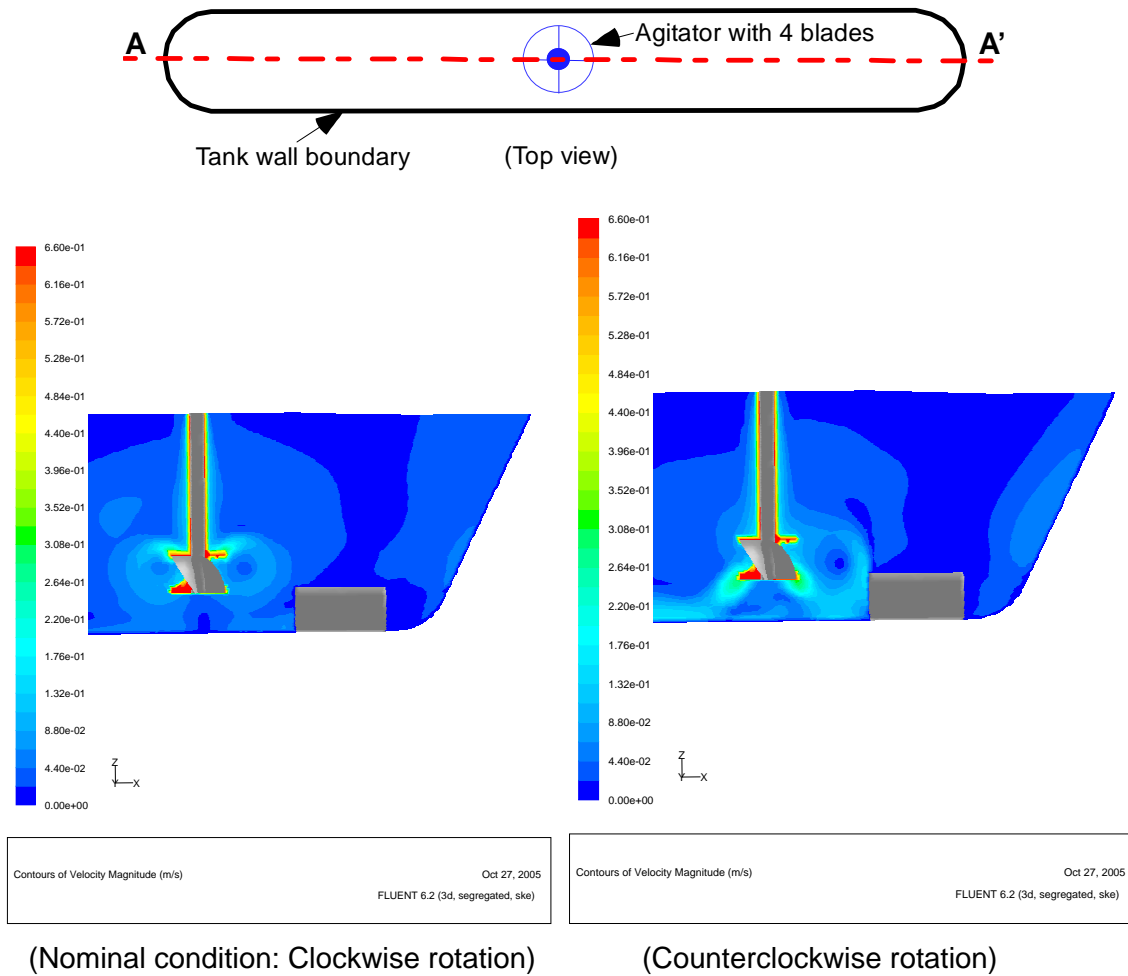


Figure 11. Comparison of velocity distributions for the entire plane A-A' of the flat tank with 15-liter liquid level and 1750 rpm agitator speed, showing that the red zone has the velocity magnitude higher than the critical velocity required for lifting up the basket from the tank floor



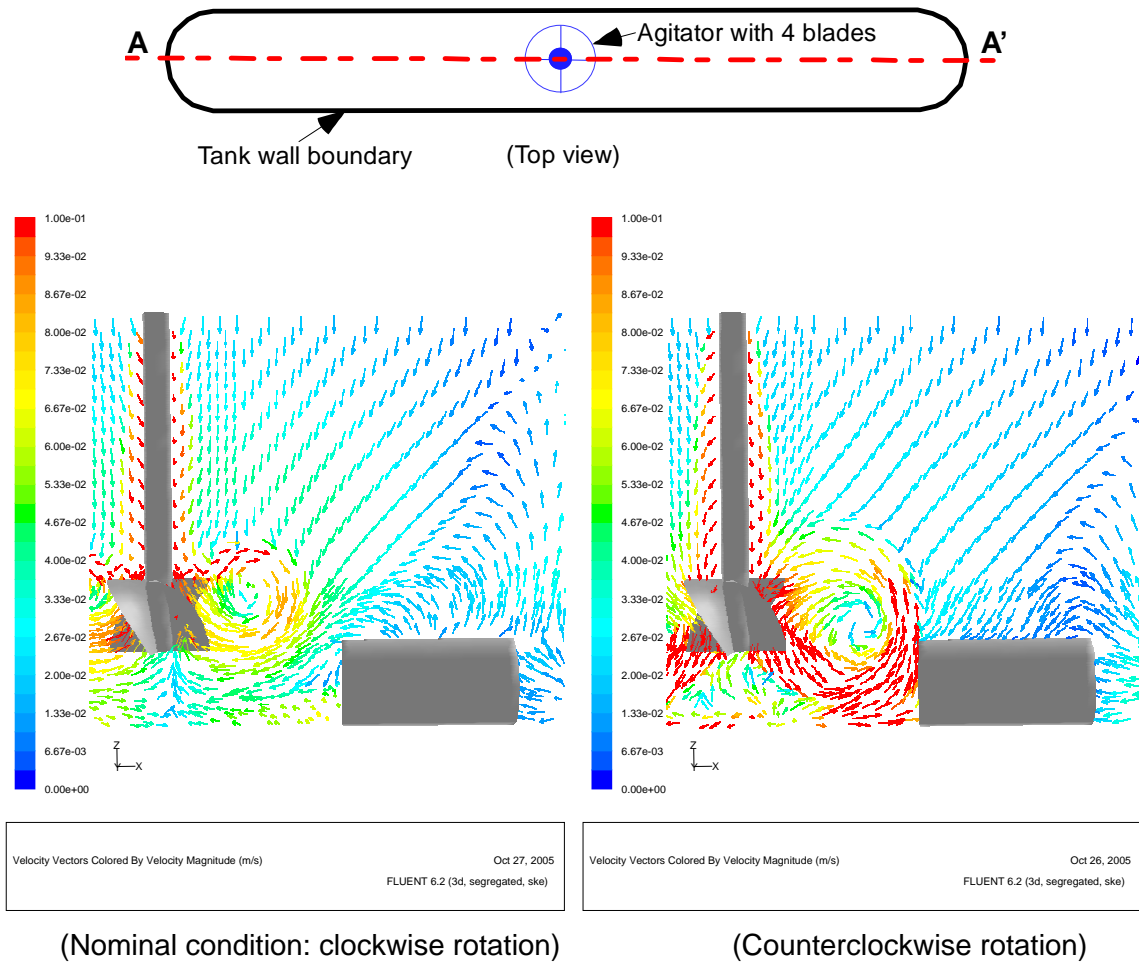


Figure 12. Comparison of flow patterns for the entire plane A-A' of the flat tank with 15-liter liquid level and 1750 rpm agitator speed, showing that the red zone has the velocity higher than 0.1 m/sec (0.33 ft/sec)

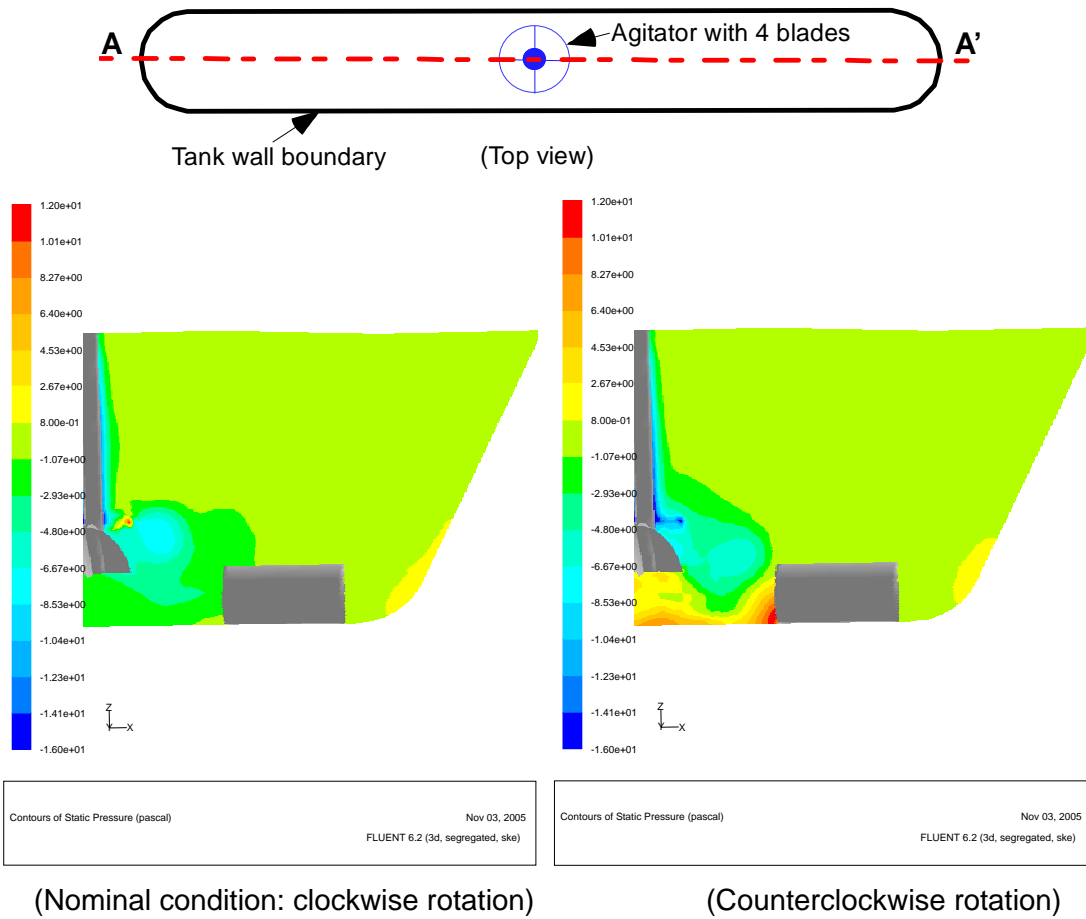


Figure 12a. Comparison of pressure distributions near the basket area for the entire plane A-A' of the flat tank with 15-liter liquid level and 1750 rpm agitator speed

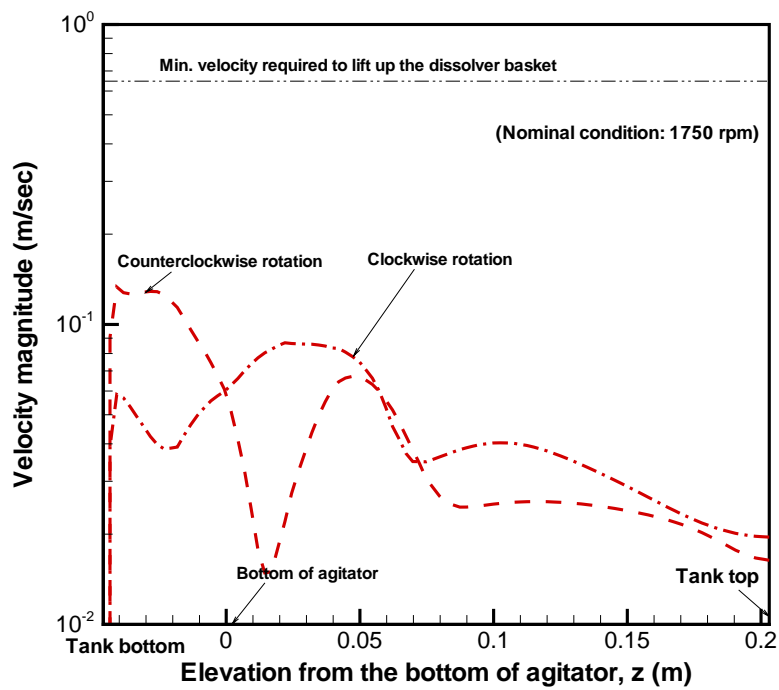
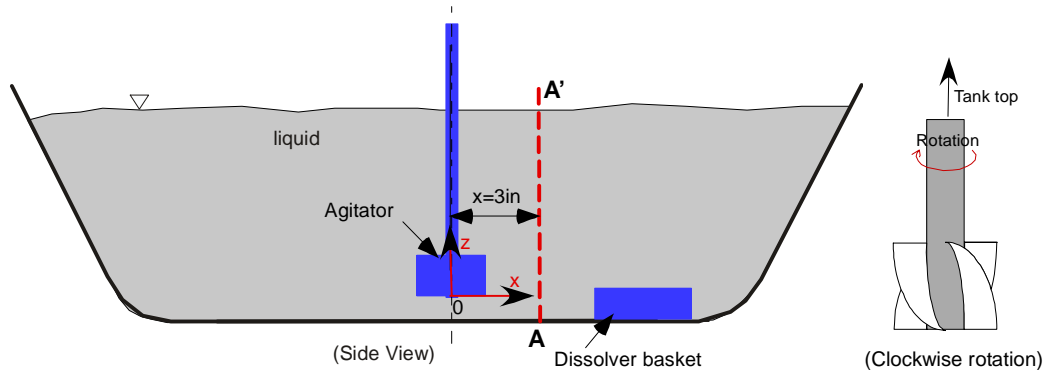
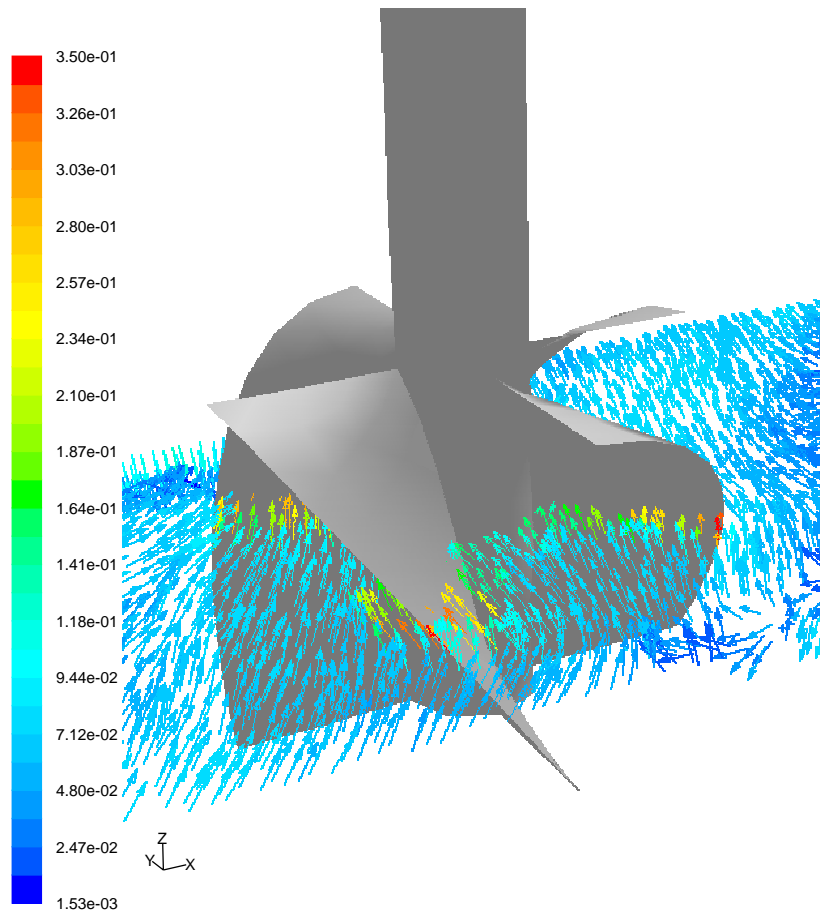
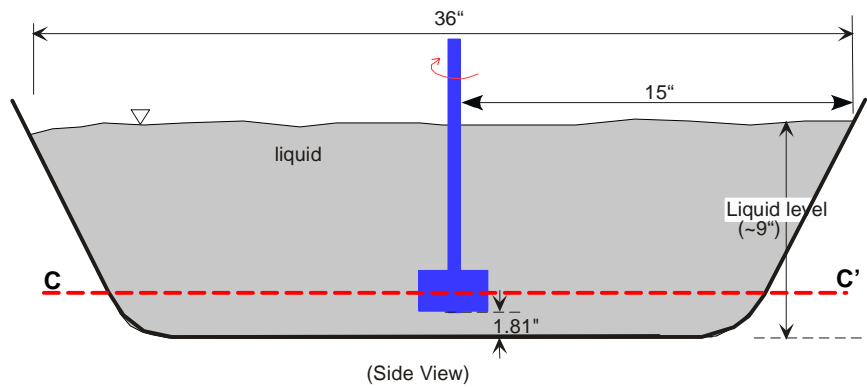
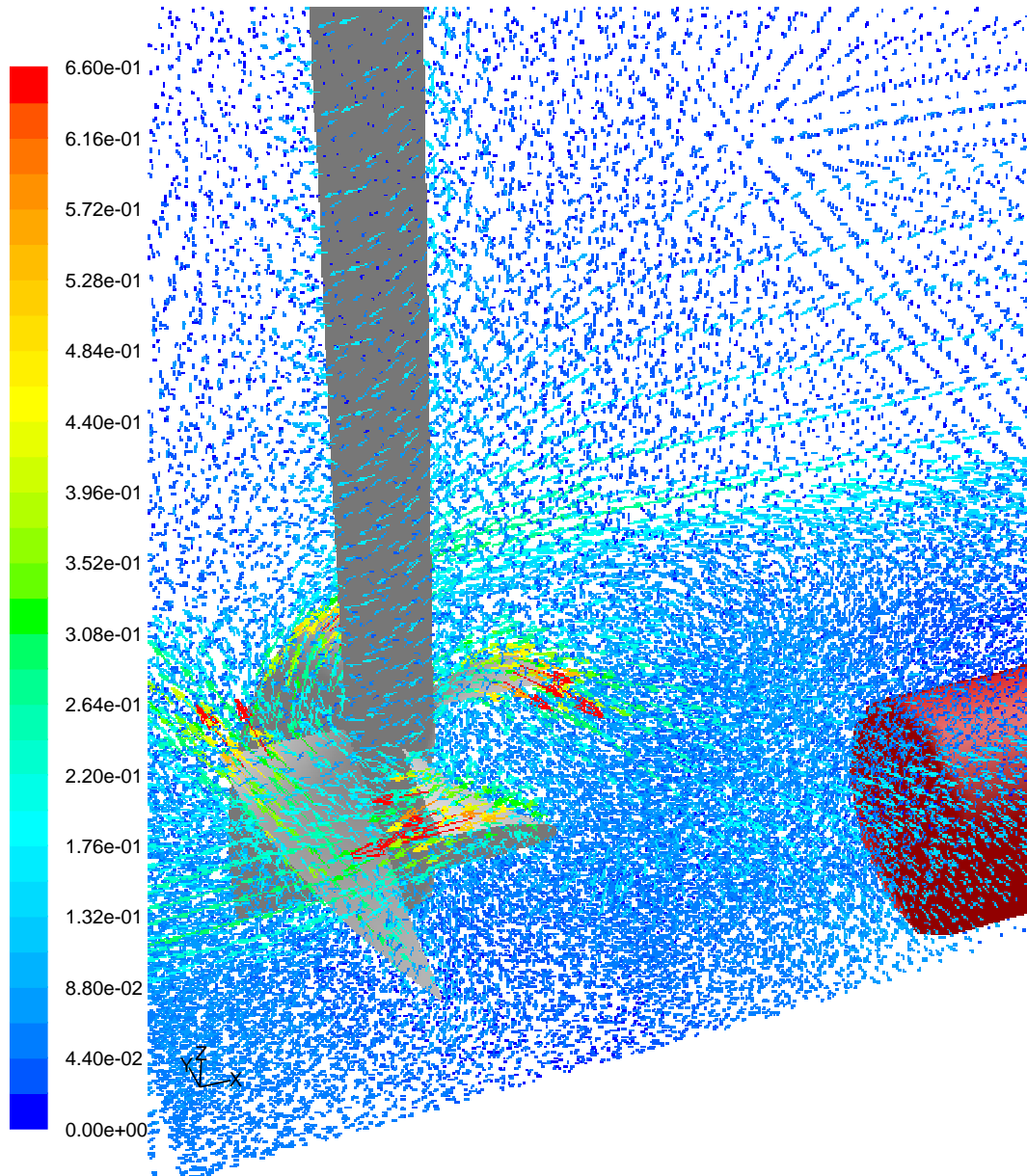


Figure 13. Comparison of velocity distributions between clockwise and counterclockwise agitator rotations along the vertical line A-A' for the nominal conditions of 1750 rpm and 15-liter tank level



Velocity Vectors Colored By Velocity Magnitude (m/s) Oct 04, 2005  
FLUENT 6.2 (3d, segregated, ske)

Figure 14. Velocity vector plot on the horizontal plane crossing the blade for the reference case shown in Table 1 (15-liter tank level and 1750 rpm agitator speed)



Velocity Vectors Colored By Velocity Magnitude (m/s)

Oct 04, 2005

FLUENT 6.2 (3d, segregated, ske)

Figure 15. Three-dimensional velocity vector plot near the agitator blade and dissolver basket from the top of the tank for the reference case shown in Table 1 (15-liter tank level and clockwise 1750 rpm agitator speed)

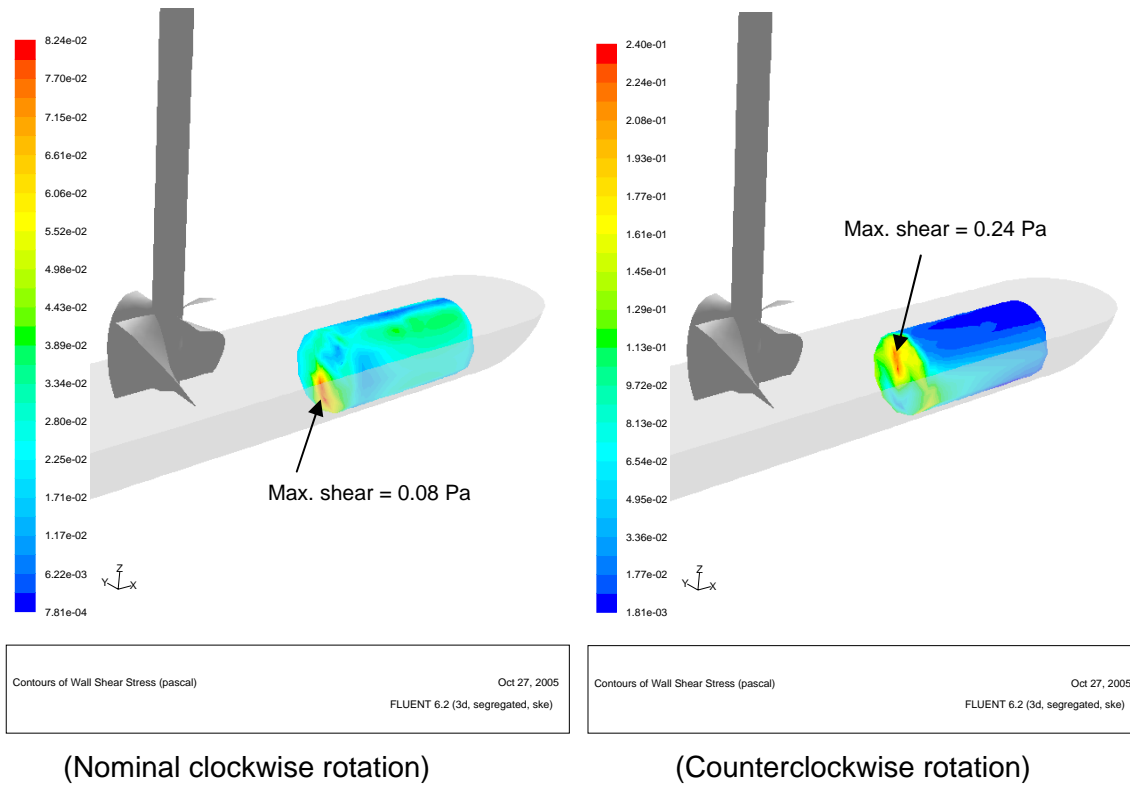
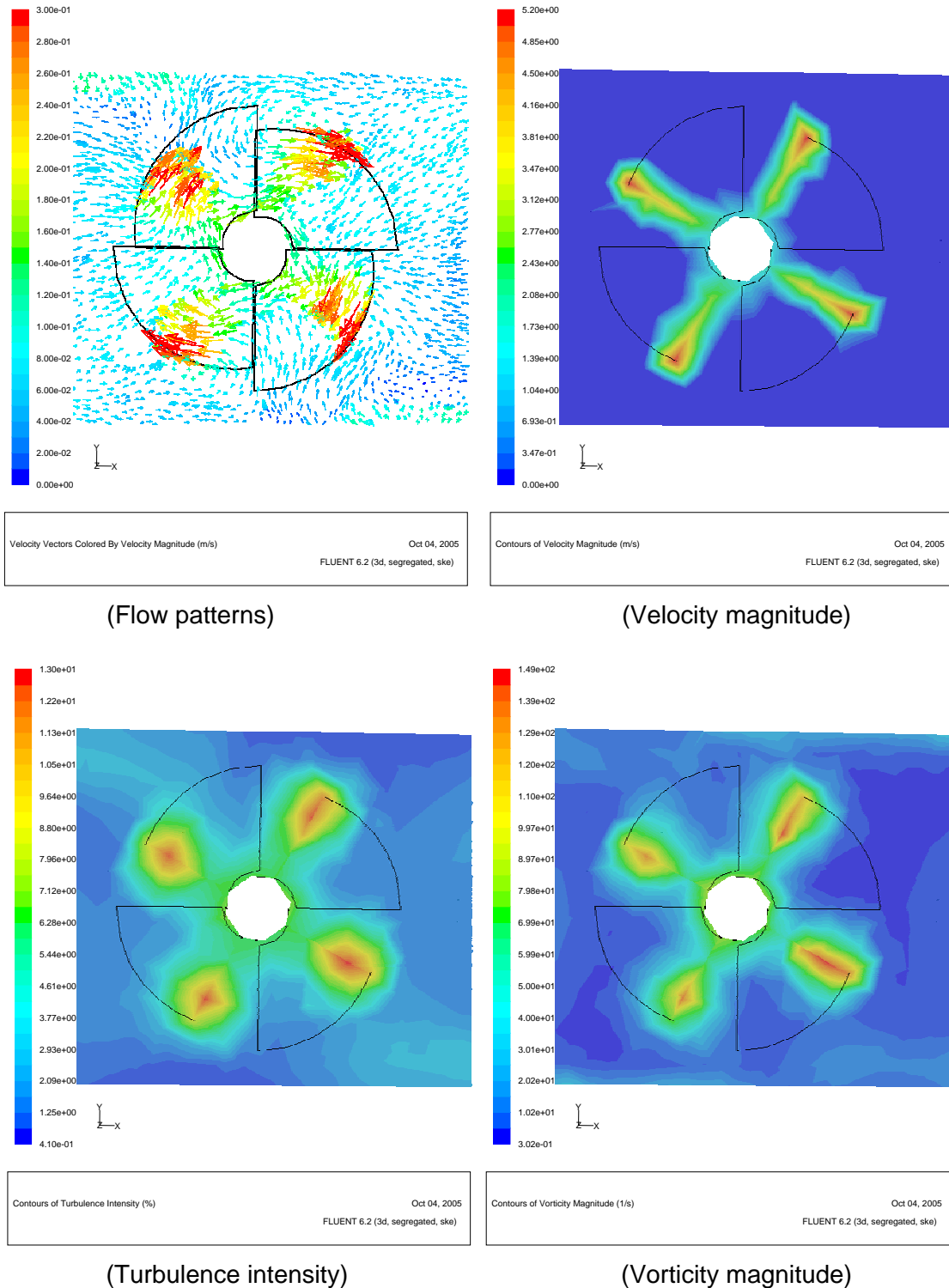


Figure 16. Comparison of wall shear distributions on the surface of the dissolver basket located near the tank bottom for two potential rotating directions of the 1750 rpm agitator submerged in 15-liter tank level, showing that the red region has maximum shear stress (Minimum wall shear required for lifting up the basket due to the fluid motion is about 45 Pa).



(Flow patterns)

(Velocity magnitude)

(Turbulence intensity)

(Vorticity magnitude)

Figure 17. Flow patterns and contour plots for some physical parameters due to the clockwise rotations of the agitator on the horizontal plane crossing the vertical center of the four-blade agitator for the nominal case (clockwise 1750 rpm agitator speed and 15-liter tank level)

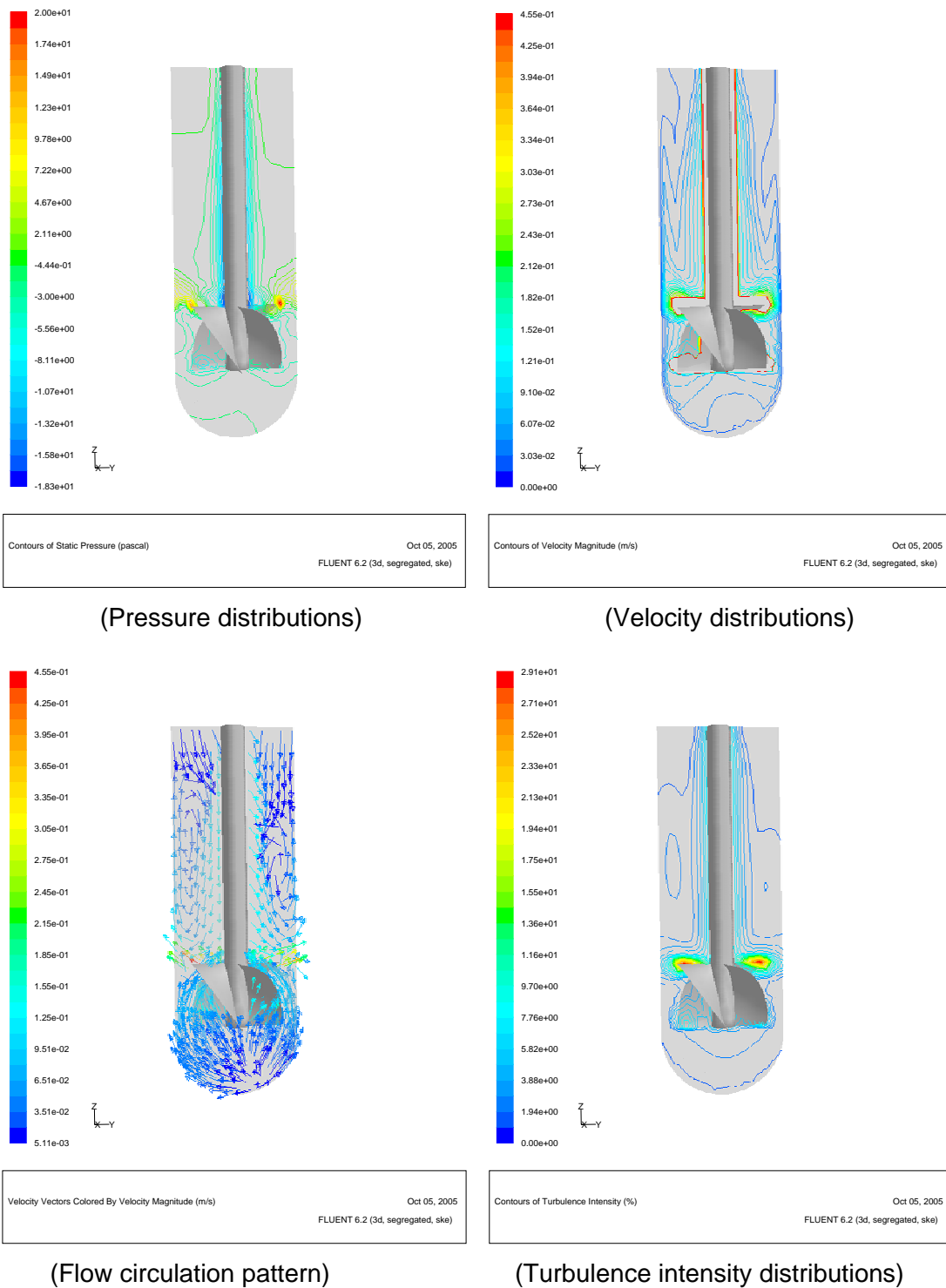


Figure 18. Flow patterns and spatial distributions of physical parameters associated with flow circulation pattern and mixing characteristics for the plane crossing the vertical center of the clockwise 1750 rpm mixing agitator submerged in the tank with 15-liter liquid level.



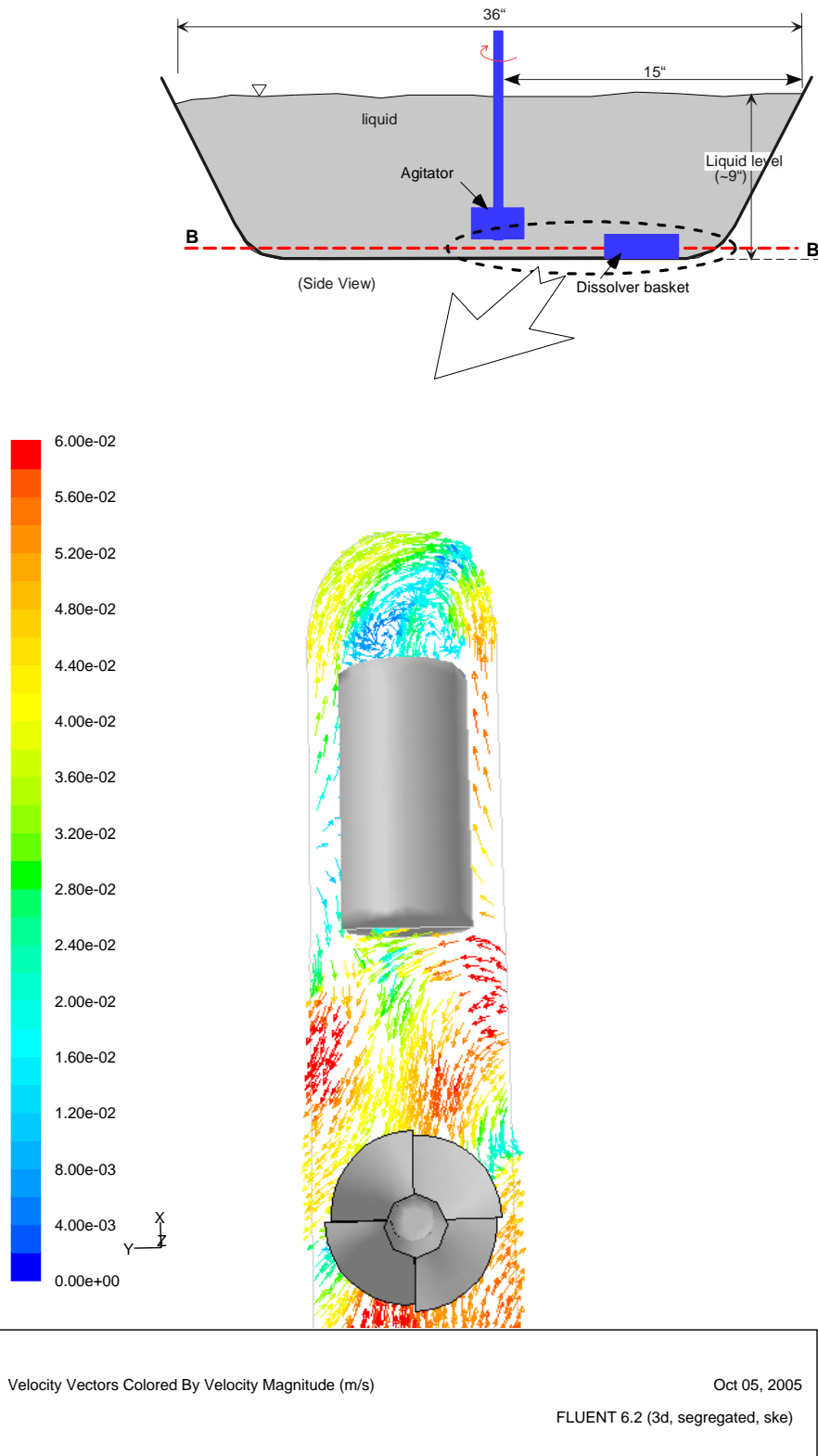


Figure 19. Flow circulation patterns for the plane crossing the center line B-B' of the dissolver basket during the mixing operation of the clockwise 1750 rpm agitator submerged in the tank with 15-liter liquid level.

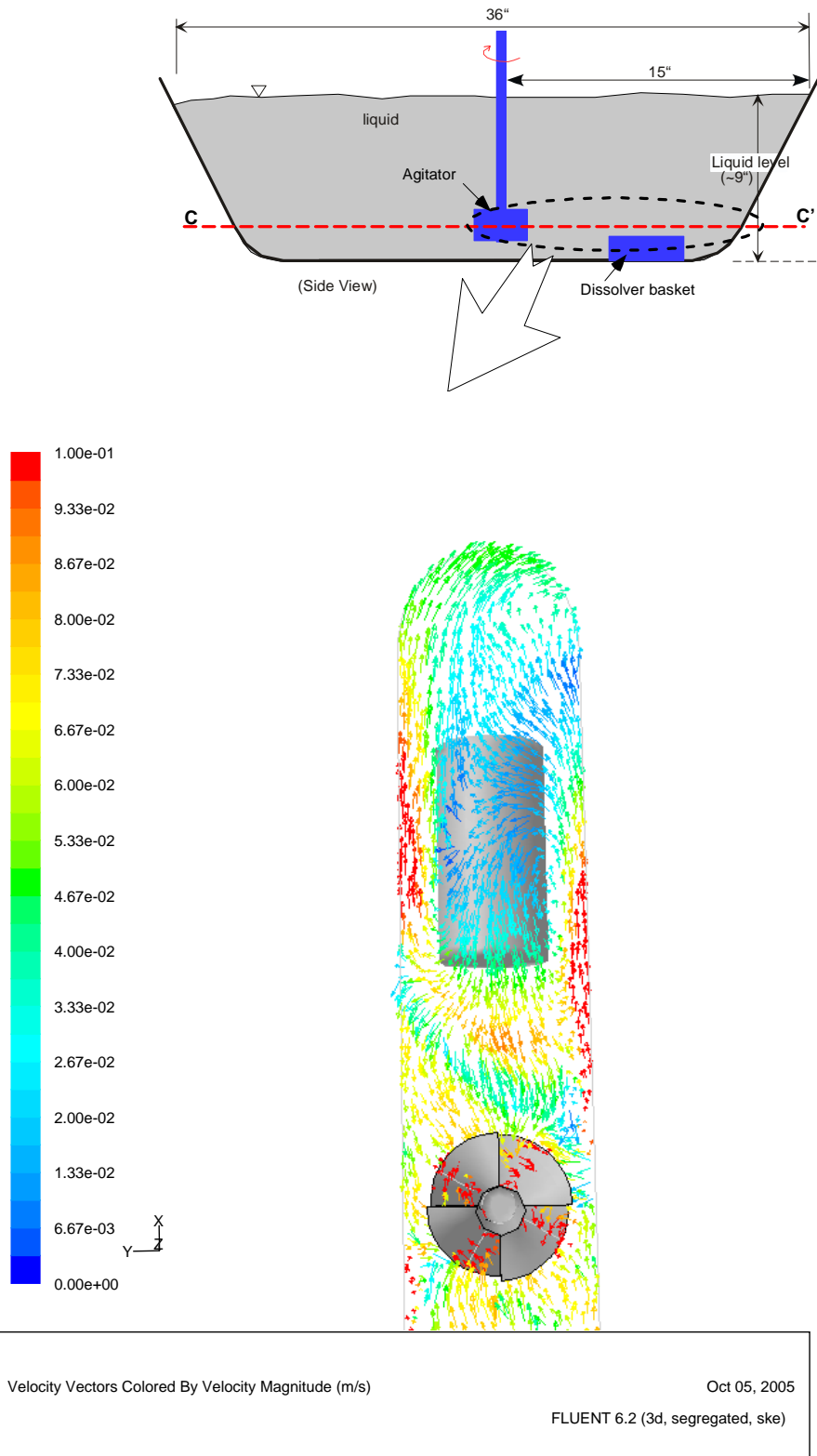
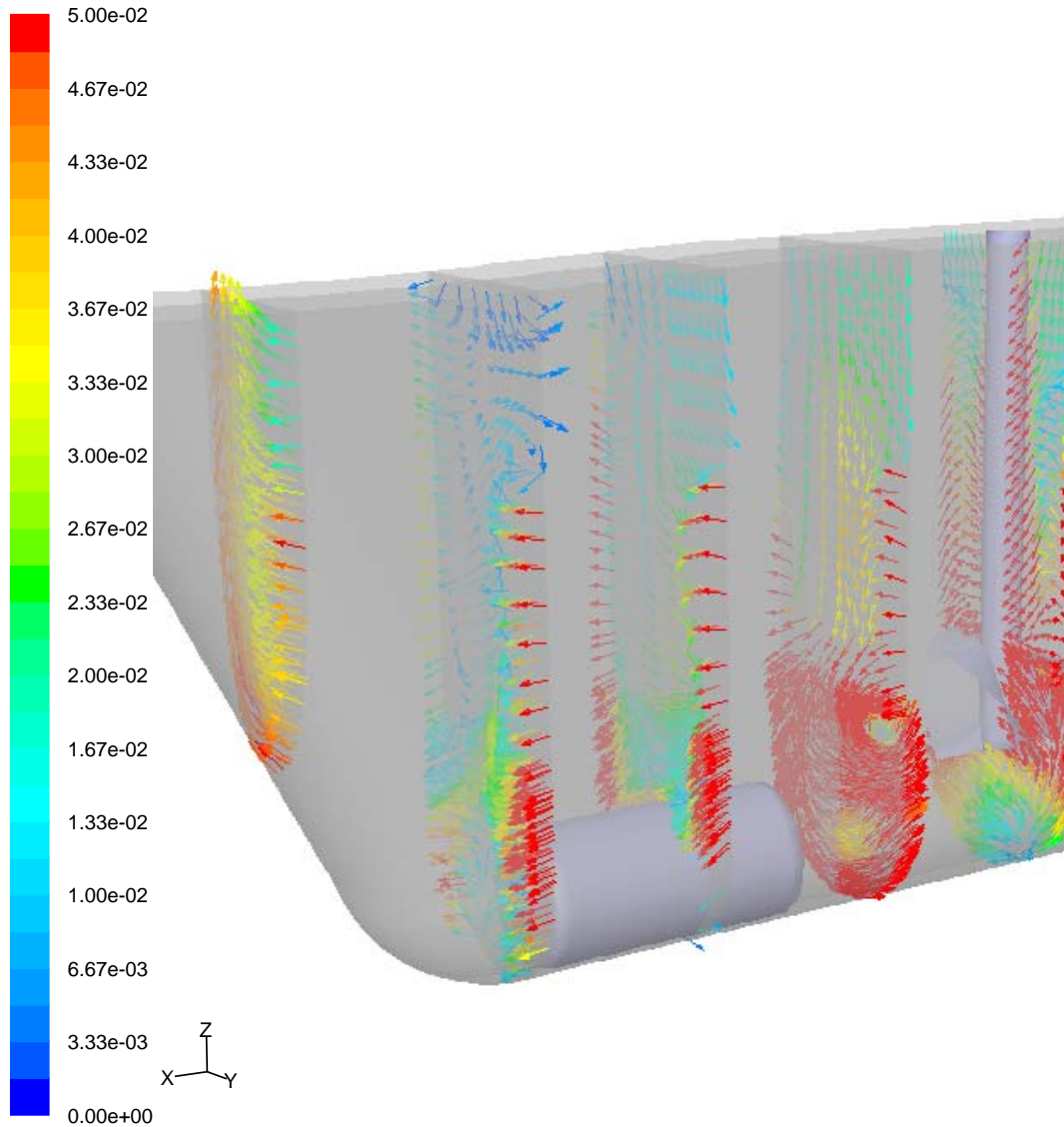


Figure 20. Flow circulation patterns and characteristics for the horizontal plane crossing the center line C-C' of the clockwise 1750 rpm mixing agitator submerged in the tank with 15-liter liquid level.

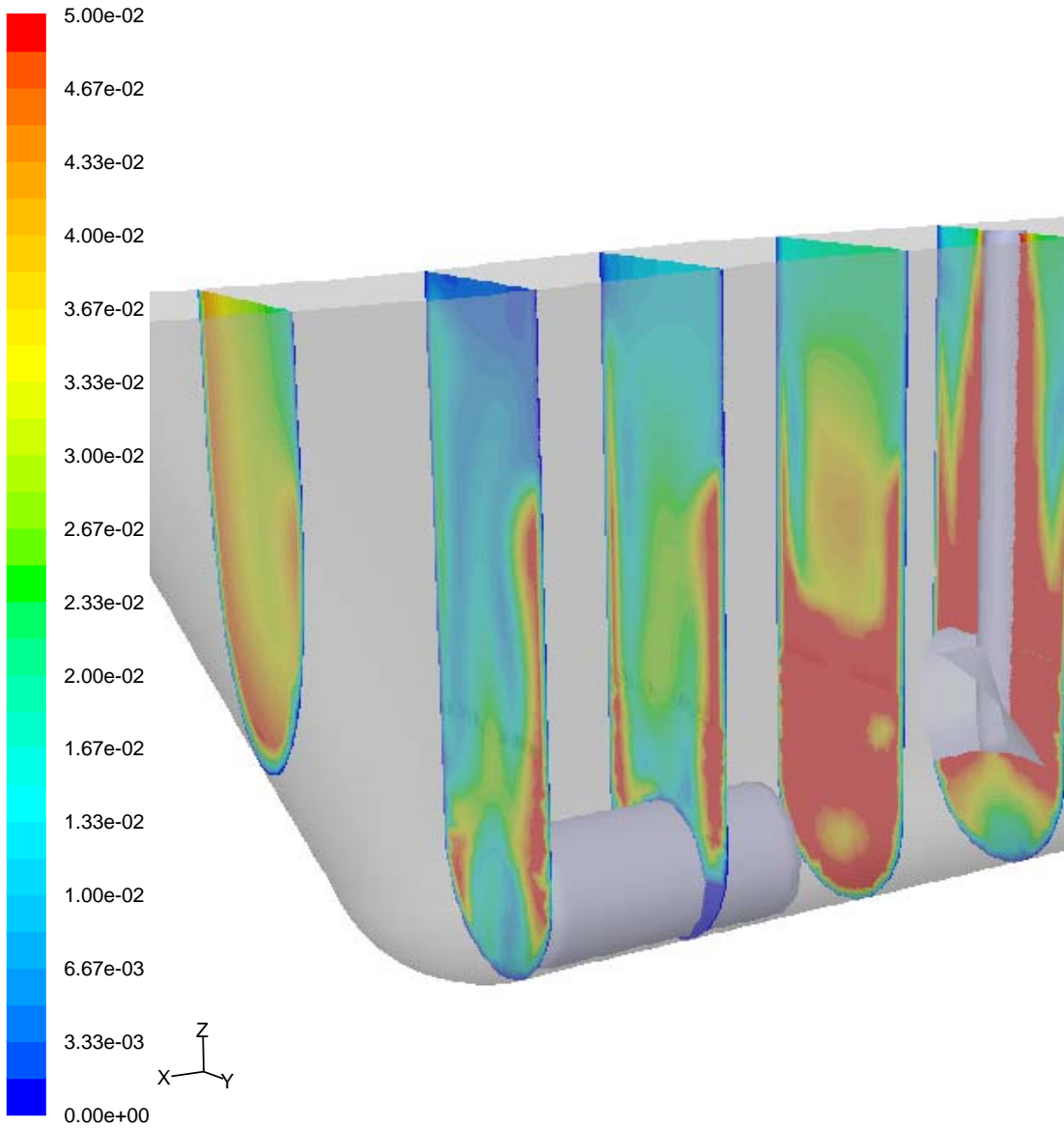


Velocity Vectors Colored By Velocity Magnitude (m/s)

Oct 05, 2005

FLUENT 6.2 (3d, segregated, ske)

Figure 21. Velocity vector plots for the planes at several different distances ( $x = 0''$ ,  $3''$ ,  $6''$ ,  $8.75''$ , and  $12''$ ) from the clockwise rotated agitator located inside the flat tank (1750 rpm agitator speed with 15-liter tank level).

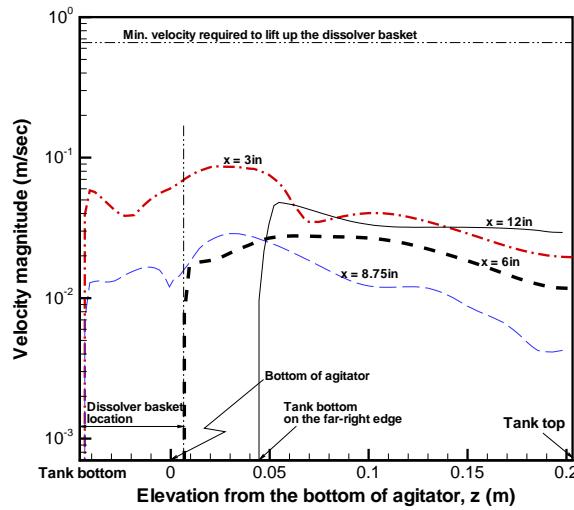
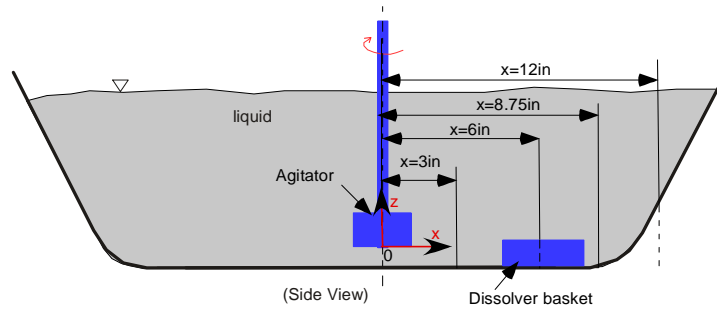


Contours of Velocity Magnitude (m/s)

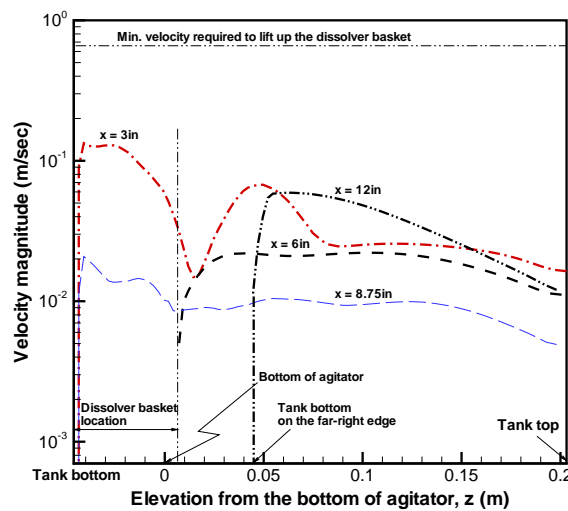
Oct 05, 2005

FLUENT 6.2 (3d, segregated, ske)

Figure 22. Velocity distributions for the planes at several different distances ( $x = 0''$ ,  $3''$ ,  $6''$ ,  $8.75''$ , and  $12''$ ) from the clockwise rotated agitator located inside the flat tank (1750 rpm agitator speed with 15-liter tank level).



(Nominal clockwise rotation)



(Counterclockwise rotation)

Figure 23. Comparison of velocity distributions between the two rotational directions along the vertical direction from the tank bottom for various horizontal distances from the 1750-rpm helical agitator submerged in the flat tank with 15-liter liquid level

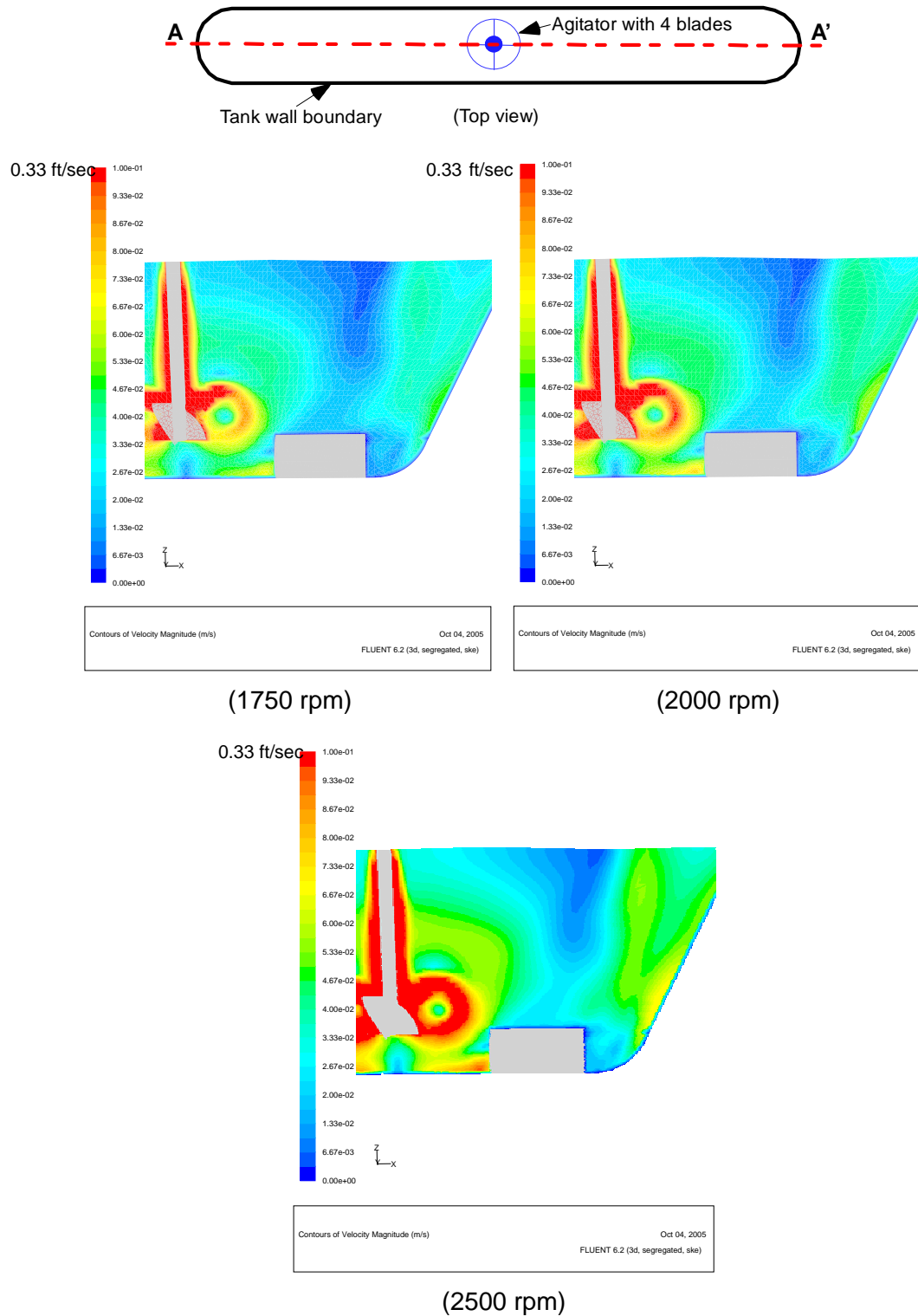


Figure 24. Velocity distributions near the dissolver basket at the vertical plane crossing the line A-A' for different speeds of the clockwise rotated agitator submerged in 2-liter tank level showing the red zone to be larger than 0.33 ft/sec (min. velocity required for lifting up one dissolver basket is about 2.17 ft/sec)

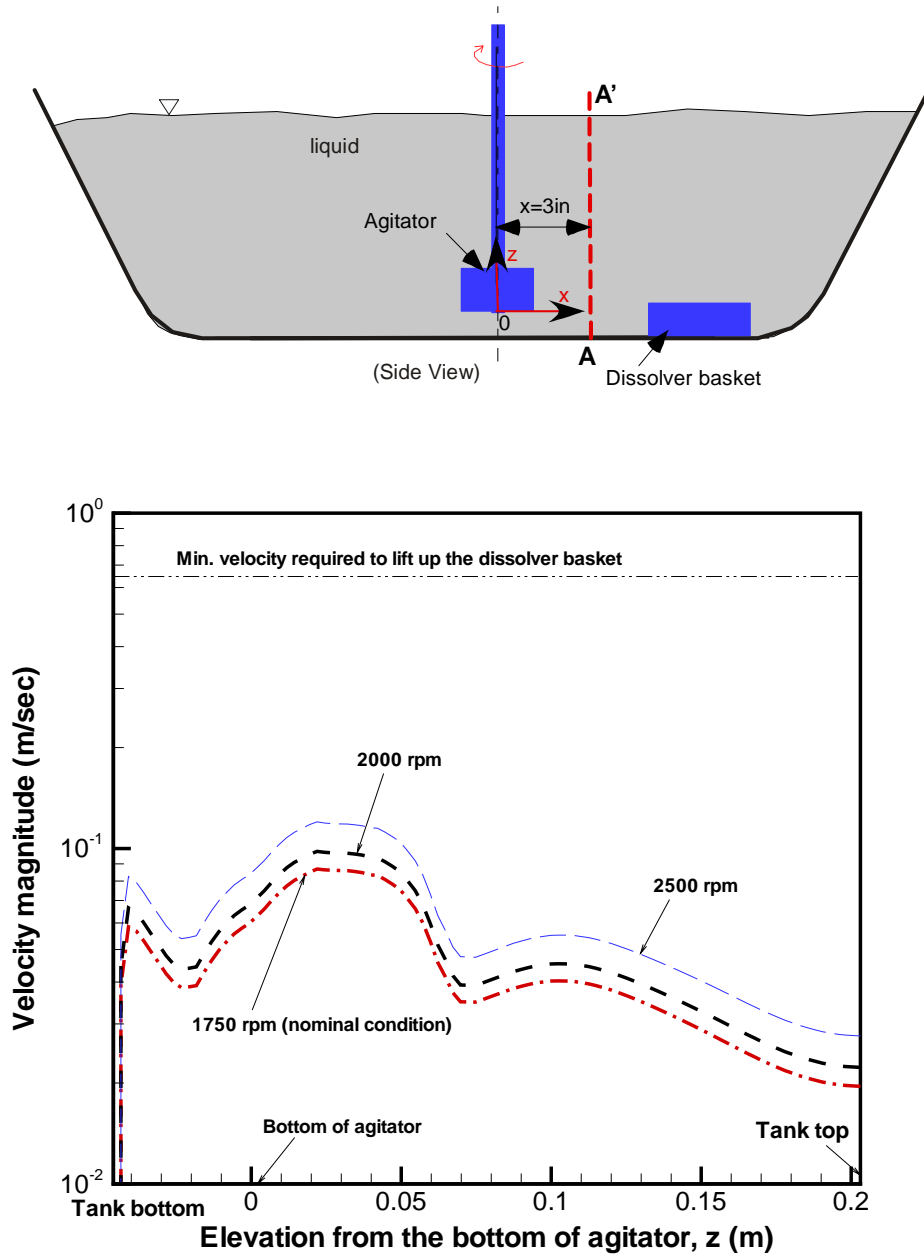


Figure 25. Velocity distributions along the vertical line A-A' for different agitator speeds at the horizontal distance of 3 inches from the agitator submerged in the flat tank filled with 15-liter liquid level (clockwise rotated agitator)

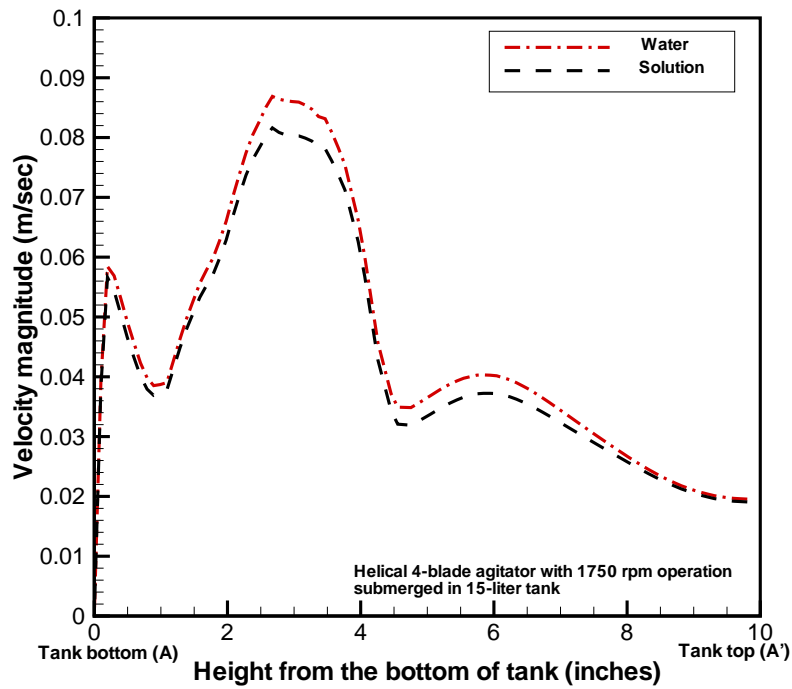
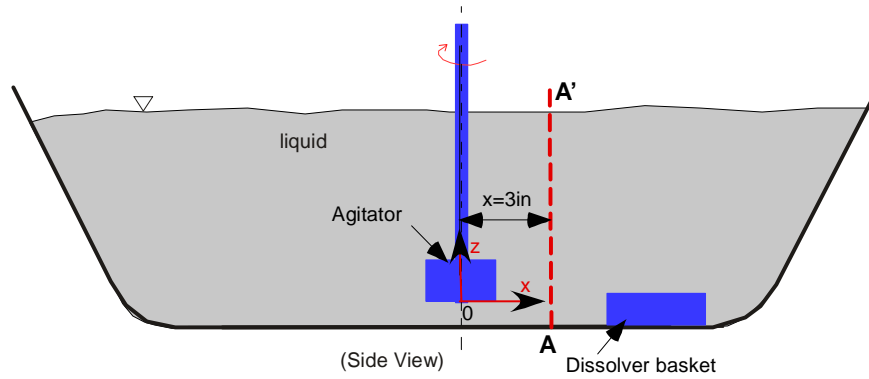


Figure 26. Comparison of velocity distributions between water and solution along the vertical line A-A' for helical 4-blade agitator at the horizontal distance of 3 inches under the 1750 rpm agitator operation in the flat tank filled with 15-liter liquid level (clockwise rotated agitator)



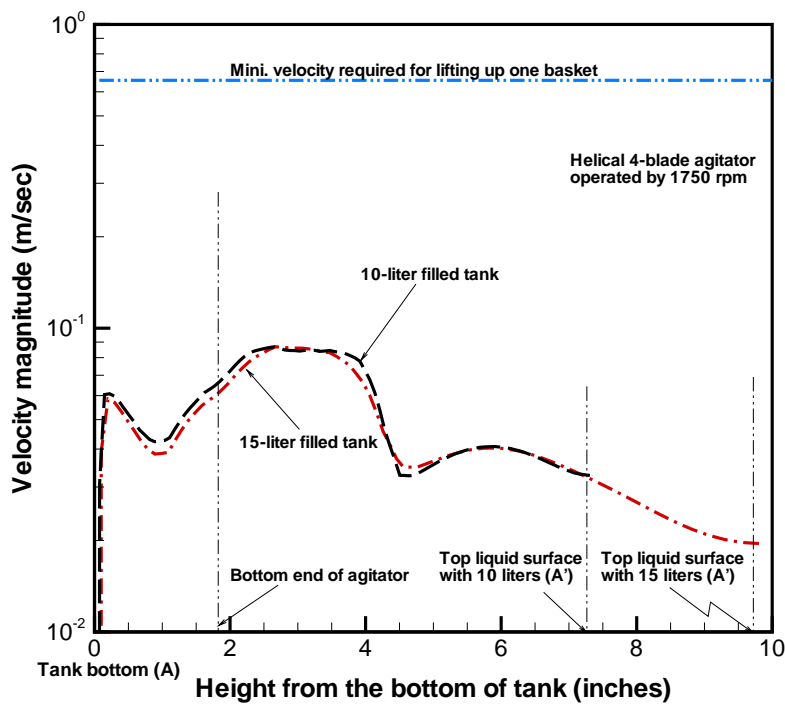
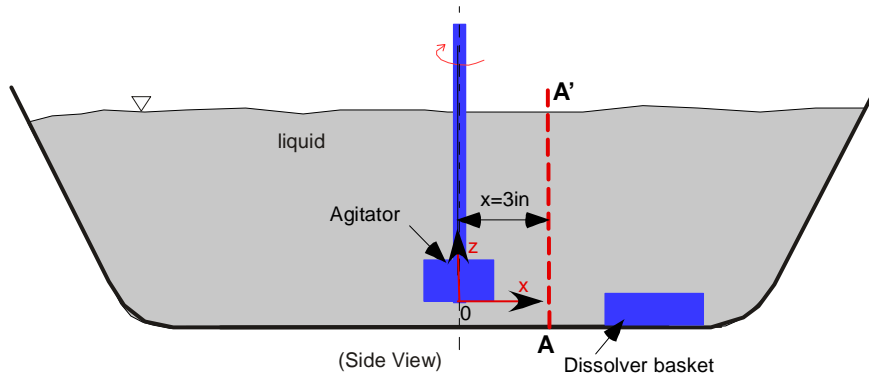


Figure 27. Comparison of velocity distributions between two different water levels along the vertical line A-A' for helical 4-blade agitator at the horizontal distance of 3 inches under the 1750 rpm agitator operation in the flat tank filled with 10-liter and 15-liter liquid levels (clockwise rotated agitator)

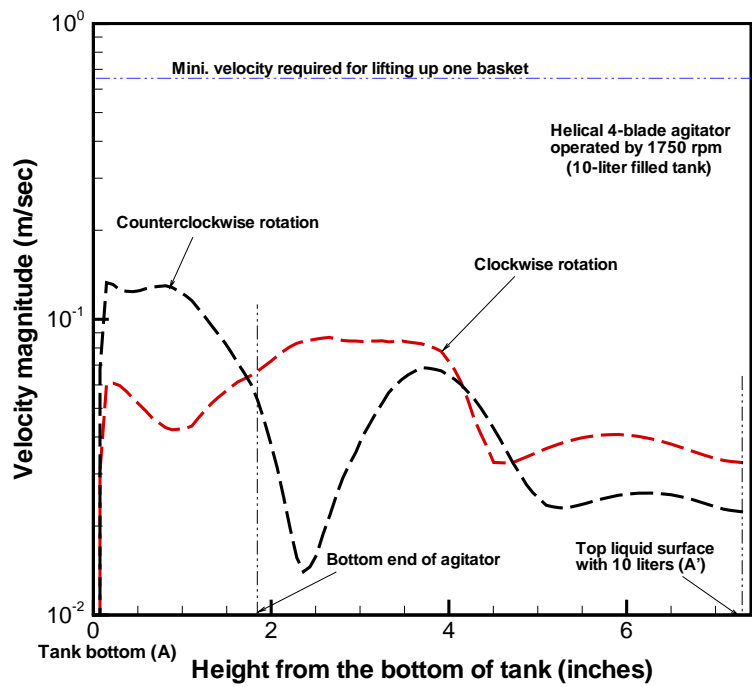
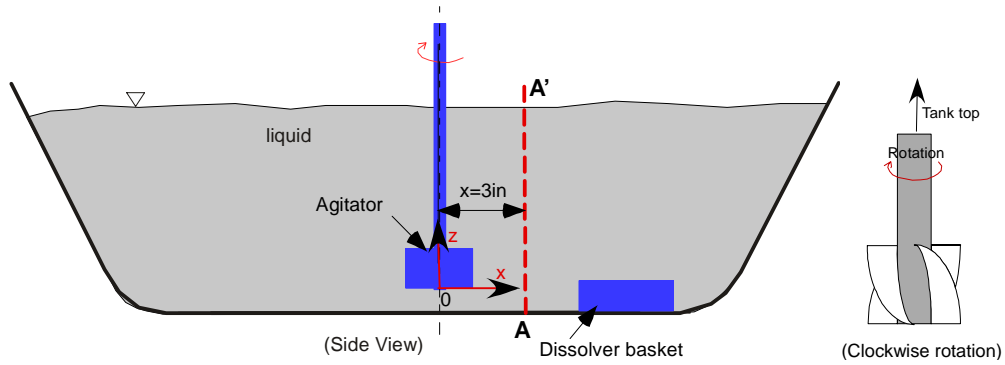


Figure 28. Comparison of velocity distributions between two different rotating directions of agitator along the vertical line A-A' for helical 4-blade agitator at the horizontal distance of 3 inches under the 1750 rpm agitator operation in the flat tank filled with 10-liter liquid level

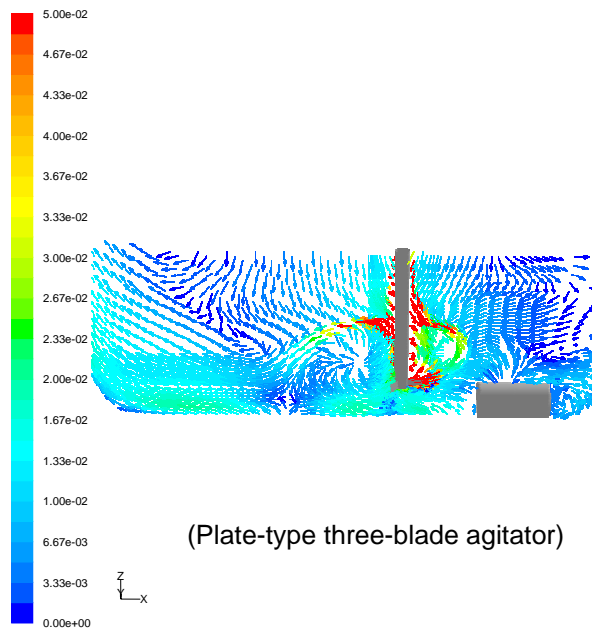
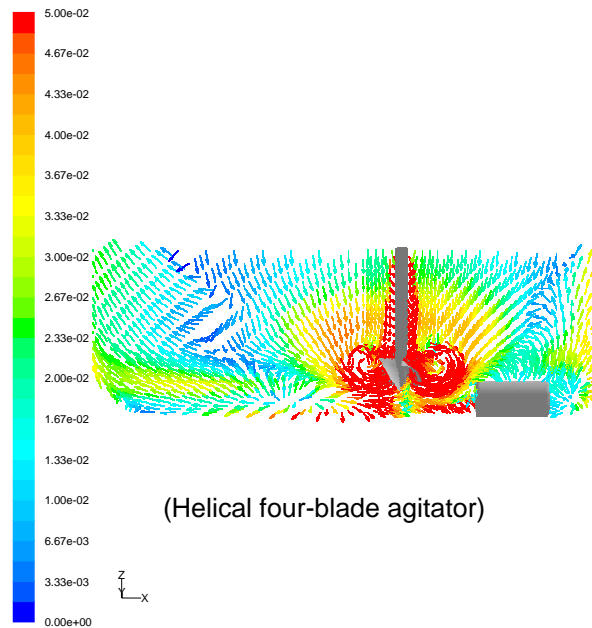
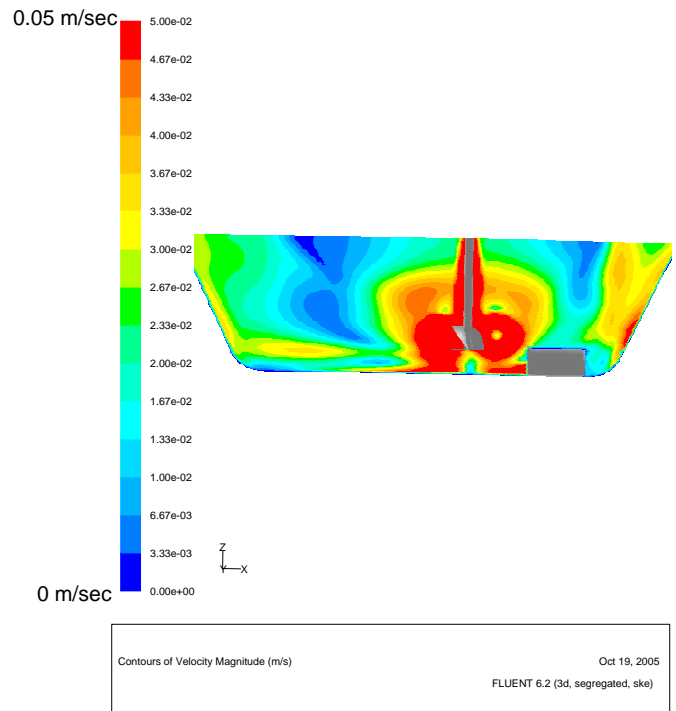
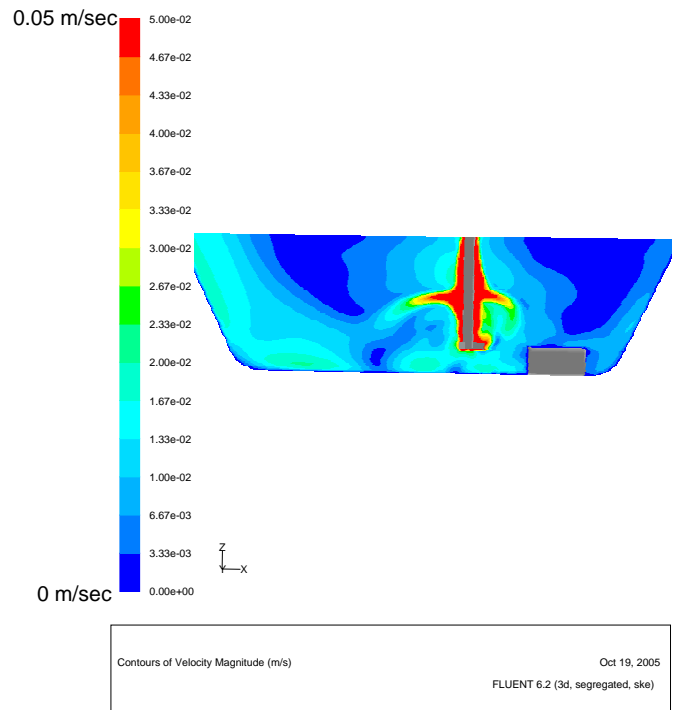


Figure 29. Comparison of velocity flow patterns between two different shapes of the agitators with 1750 rpm operations at the vertical center plane under the same color scale



(Helical 4-blade agitator submerged in 15-liter water tank)



(Radial 3-blade agitator submerged in 15-liter water tank)

Figure 30. Comparison of velocity contours between two different shapes of the agitators with 1750 rpm operations at the vertical center plane under the same color scale (clockwise rotated agitators)

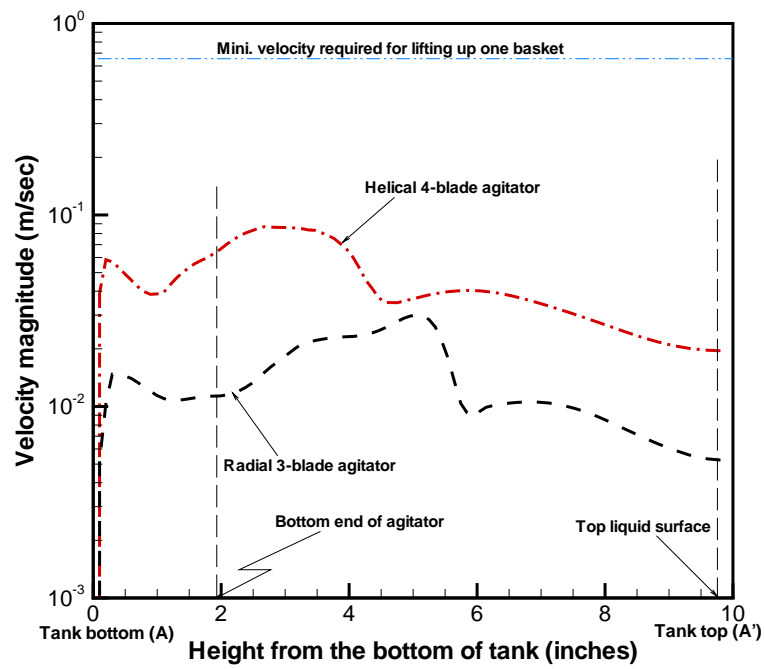
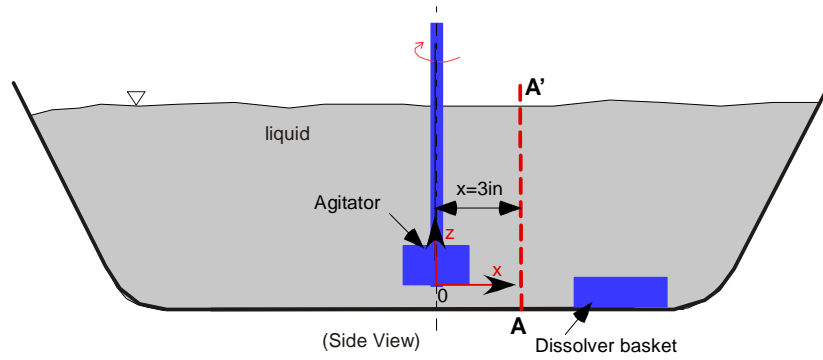
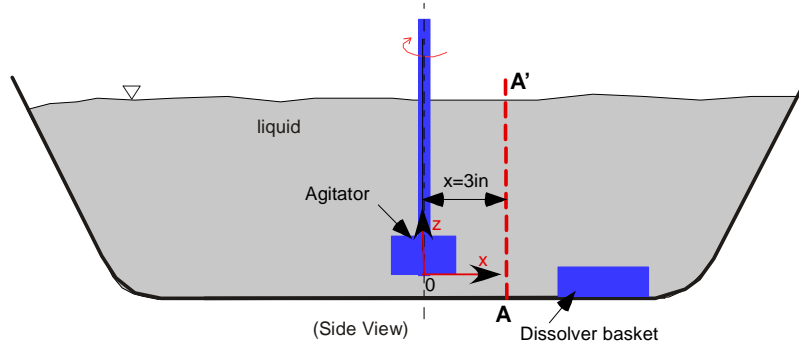


Figure 31. Velocity distributions along the vertical line A-A' for different agitator shapes at the horizontal distance of 3 inches under the nominal operating conditions

Table 4. Comparison of average local velocity magnitudes for three different speeds of the agitator between two types of agitators at the 3-inch distance from the agitator submerged in 15-liter tank level



Agitator speed (rpm)	Average Local Velocity magnitude at the vertical line A-A' (m/sec)		Min. critical velocity for lifting up one dissolver basket (m/sec)
	Helical four-blade agitator for the nominal reference case	Flat three-blade agitator for sensitivity run	
1750	0.051 (0.045)*	0.014	0.66
2000	0.058 (0.051)*	0.016	
2500	0.071 (0.064)*	0.020	

Note:\* For counterclockwise rotation of agitator

Table 5. Summary of results for different rotational speed of helical four-blade agitator submerged in 15-liter water or solution

Agitator speed (rpm)	Fluid	Max. local velocity magnitude (m/sec)		Critical velocity for one basket lift-up (m/sec)	Max. shear magnitude on basket surface (Pa)	Critical shear for one basket lift-up (Pa)
		Near agitator	Near basket			
1750	water	5.26	0.05 (0.15)*	0.66	0.08 (0.24)*	44.5
	Solution <sup>+</sup>	5.26	0.05 (0.14)*		0.06 (0.21)*	
2000	water	6.01	0.08 (0.17)*	0.66	0.10 (0.27)*	44.5
	Solution <sup>+</sup>	6.01	0.07 (0.16)*		0.07 (0.26)*	
2500	water	7.41	0.11 (0.21)*	0.66	0.12 (0.34)*	44.5
	Solution <sup>+</sup>	7.41	0.09 (0.20)*		0.09 (0.33)*	

Note:\* For counterclockwise helical agitator rotation when observed from the tank top

<sup>+</sup> As provided in Table 1

Table 6. Summary of results for different rotational speed of flat-plate three-blade agitator submerged in 15-liter tank

Agitator speed (rpm)	Fluid	Max. local velocity magnitude (m/sec)		Critical velocity for one basket lift-up (m/sec)	Max. shear magnitude on basket surface (Pa)	Critical shear for one basket lift-up (Pa)
		Near agitator	Near basket			
1750	water	5.25	0.012	0.66	0.012	44.5
2000	water	6.00	0.014	0.66	0.015	44.5
2500	water	7.41	0.018	0.66	0.021	44.5

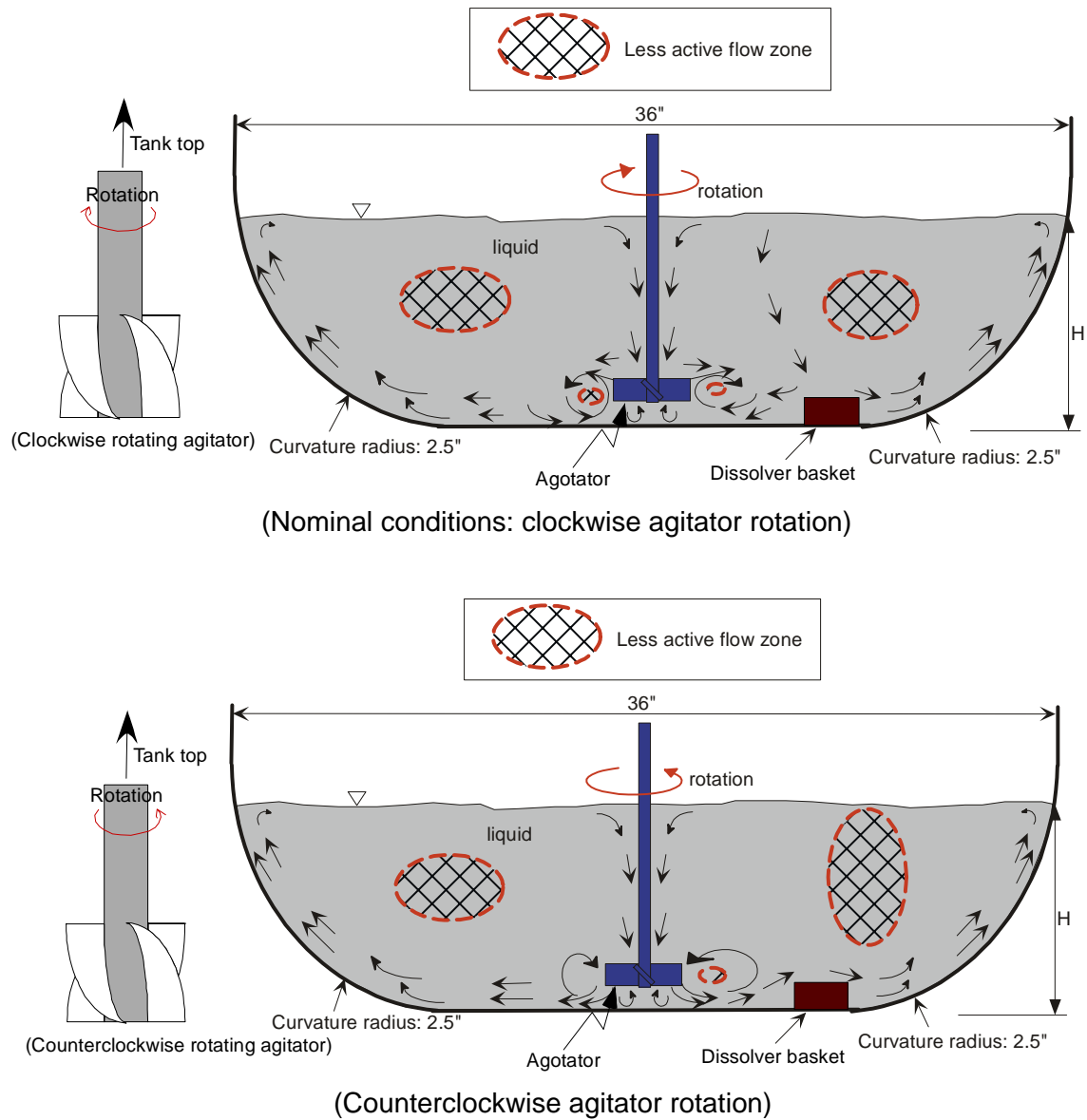


Figure 32. Flow circulation patterns and characteristics for the turbulent helical four-blade agitator submerged in the flat HB-Line tank with flow obstacle of dissolver basket.



## 4. Conclusions

Flow pattern calculations for potential operating conditions of a helical pitched four-blade agitator in the HB-line flat tank have been performed to estimate flow patterns and to determine whether nominal agitator speed can keep a dissolver basket from contacting the agitator blade during the potential operating conditions with different types of agitators and tank levels. Velocity and shear stress criteria were developed to assess the ability of liquid flow to lift up a dissolver basket settled on the bottom surface of the tank and touch the agitator blade. The modeling results will help determine acceptable agitator speeds and tank liquid levels to ensure that the dissolver basket is kept from contacting the agitator blade during HB-Line dissolver tank operations.

The nominal calculations and a series of sensitivity runs were performed to examine the impact of flow patterns on the lifting behavior of the dissolver basket. Three different agitator speeds of 1750, 2000, and 2500 rpm and two different tank levels of about 10 and 7.4 inches, corresponding to 15 and 10 liters were evaluated. A three-dimensional CFD approach was used with a two-equation turbulence model and multiple reference frames. Two different types of the agitator blades were also considered in the model. Free surface motion was assumed to be negligible compared to forced convective motion for the operating conditions evaluated. The top liquid surface was assumed to be stationary at atmospheric pressure since the tank levels considered here were high enough to avoid air pull-through due to vortex formation near the tips of the agitator blades. According to the literature information [4], about 6 inches of tank level is required for the prevention of air pull-through from the free surface under the potential operating conditions. No-slip boundary conditions were used at the blade surface and the tank walls. Rotational motion of the agitator was simulated by using a rotating reference frame with respect to the adjacent fluid media.

When local turbulent flow at a higher agitator speed reaches the critical condition to pick up the basket from the tank floor and suspend it, the basket can touch the agitator blades during the tank mixing, which is not desirable in terms of mixing performance. The nominal calculations and a series of sensitivity runs were performed to examine the impact of flow patterns on the lifting behavior of the dissolver basket.

The main conclusions are as follows:

- The modeling results demonstrate that the flow patterns driven by the agitators considered here are not strong enough to lift up the dissolver basket for the agitator speeds up to 2500 rpm. Table 5 and Table 6 summarize the results.
- The maximum fluid velocity discharged by the agitator was found to be proportional to the rotational speed of the agitator. These results were consistent with the literature information over a range of agitator speeds.
- When the helical four-blade agitator was used for tank mixing, local velocity magnitudes near the basket for the counterclockwise rotating case were much larger than those of the clockwise motion under the same operating conditions as shown in Table 5. However, it was noted that velocity magnitudes averaged over the entire region were about the same magnitude for the two cases because of the same agitator power dissipation rate into the tank fluid.

- When tank fluid is about 50% heavier than the nominal fluid of water, the calculated results show that local velocity magnitude near the dissolver basket is decreased by about 10%, compared to that of the nominal conditions.
- Two different tank levels corresponding to 10 and 15 liters tank volumes were evaluated to estimate the sensitivity of flow patterns to the rotational speed of the agitator. Local velocity magnitude for the lower tank level of the 10-liter fluid volume is slightly higher than the higher one under the nominal operating conditions other than the tank level. These results are consistent with the literature information.
- Helical four-blade agitator was used as one of the reference operating conditions. Flat-plate three-blade agitator was also used to estimate the sensitivity of local flow patterns. The modeling results clearly show that local velocity magnitudes for the three-blade agitator are at maximum three times smaller than the helical four-blade one.

## 5. References

1. Technical Task Request (TTR), NMMD-HTS-1917, August 23, 2005.
2. Rosa Hill, "Weight of Basket and Chain", E-mail, September 26, 2005.
3. Rosa Hill, "Density and Viscosity Information", E-mail, October 12, 2005.
4. S. Y. Lee, "Agitator Mixing Analysis in a HB-Line Flat Tank", WSRC-TR-2002-00219, May 2002.
5. FLUENT, Fluent, Inc., Lebanon, New Hampshire, 1998.
6. F. D. Miller and J. H. Rushton, "A Mass Velocity Theory for Liquid Agitation", Ind. And Eng. Chemistry, vol. 36, no. 6, pp. 499-503, 1944.
7. G. Batchelor, "Theory of Homogeneous Turbulence", p. 103, Cambridge University Press, Cambridge, 1959.
8. A. W. Hixson, "Nature and Measure of Agitation", Ind. And Eng. Chemistry, vol. 36, no. 6, pp. 488-496, June 1944.
9. G. B. Tatterson, Fluid Mixing and Gas Dispersion in Agitated tanks, McGraw-Hill, Inc., New York, 1991.
10. R. B. Richard and G. J. Carlson, "Power Absorption and Fluid Properties, Correlation with Equipment Dimensions and Fluid Properties", Chem. Eng. Progress, vol. 43, no. 9, pp. 473-480, 1947.
11. I. E. Idelchik, "Handbook of Hydraulic Resistance", 2<sup>nd</sup> Edition, Hemisphere Pub. Corp, 1986.